

# Functional metal-organic frameworks for metal removal from aqueous solutions

Herlys Viltres, Yeisy C. López, Nishesh Kumar Gupta, Carolina Leyva, Roxana Paz, Anjali Gupta & Arijit Sengupta

To cite this article: Herlys Viltres, Yeisy C. López, Nishesh Kumar Gupta, Carolina Leyva, Roxana Paz, Anjali Gupta & Arijit Sengupta (2022) Functional metal-organic frameworks for metal removal from aqueous solutions, Separation & Purification Reviews, 51:1, 78-99, DOI: [10.1080/15422119.2020.1839909](https://doi.org/10.1080/15422119.2020.1839909)

To link to this article: <https://doi.org/10.1080/15422119.2020.1839909>



Published online: 23 Nov 2020.



Submit your article to this journal [↗](#)



Article views: 435



View related articles [↗](#)



View Crossmark data [↗](#)

REVIEW



## Functional metal-organic frameworks for metal removal from aqueous solutions

Herlys Viltres<sup>a</sup>, Yeisy C. López<sup>a,b</sup>, Nishesh Kumar Gupta<sup>c,d</sup>, Carolina Leyva<sup>d,e</sup>, Roxana Paz<sup>a</sup>, Anjali Gupta<sup>e</sup>, and Arijit Sengupta<sup>f,g</sup>

<sup>a</sup>Centro De Investigación En Ciencia Aplicada Y Tecnología Avanzada, Instituto Politécnico Nacional, CDMX, Mexico; <sup>b</sup>Laboratorio De Bioninorgánica, Facultad De Química, Universidad De La Habana, Havana, Cuba; <sup>c</sup>University of Science and Technology (UST), Daejeon, Republic of Korea; <sup>d</sup>Department of Land, Water, and Environment Research, Korea Institute of Civil Engineering and Building Technology (KICT), Goyang, Republic of Korea; <sup>e</sup>Department of Chemistry, Dayalbagh Educational Institute, Agra, India; <sup>f</sup>Radiochemistry Division, Bhabha Atomic Research Center, Mumbai, India; <sup>g</sup>Homi Bhabha National Institute, Mumbai, India

### ABSTRACT

Wastewater remediation technologies are rapidly evolving to meet the increasing water demand. The need to develop efficient, low-cost, and simplistic strategies has motivated researchers to explore newer fields of material science. Owing to high thermal stability, porosity, and accessible functionalities, metal-organic frameworks (MOFs) are finding numerous applications in the domain of wastewater treatment and resource recovery. The application-oriented development of MOFs has been accepted as a novel approach for the removal and recovery of metals from waste solutions. The desired properties in MOFs could be achieved by adopting suitable synthesis or post-synthesis functionalization strategies. Here, we have reviewed differently functionalized MOFs and their application in the removal of metals from waste solutions. We have also discussed the application of MOFs in the pre-concentration and recovery of actinides from seawater. Conclusions regarding the future scope of employing MOFs in the domain of environmental remediation have been included.

### ARTICLE HISTORY

Received 16 June 2020  
Revised 6 October 2020  
Accepted 11 October 2020

### Keywords





Actinides; adsorption; functionalized MOFs; heavy metal; rare earth elements

### Introduction

The toxic nature of heavy metals has been known to mankind for ages. Uncontrolled anthropogenic activities have increased the levels of hazardous metal ions, leading to serious environmental and human damages. Unlike organic pollutants, metal ions are non-degradable and accumulate in living organisms over time. They need to be eliminated at the beginning of the anthropogenic activity cycle.<sup>[1]</sup> Another fundamental aspect is the precious metals, rare earth elements, and actinides in the biomedical, catalysis, electronics, and energy sectors. The natural reserves of said metals are scarce and unevenly distributed. With the rapid resource consumption in this century, it is expected that these resources will completely depleted soon. All these concerns have put pressure on the scientific community to develop effective methods for the removal and recovery of metals from water sources.<sup>[2]</sup> Adsorption is a simplistic, economical, and widespread approach toward the removal of heavy metals from waste solutions applied in wastewater treatment facilities. Although adsorbents like activated carbon,<sup>[3,4]</sup> biosorbents,<sup>[5,6]</sup> magnetic nanoparticles,<sup>[7]</sup> and graphene oxide<sup>[8,9]</sup> are effective in removing heavy metals they do have limitations. In some cases, these adsorbents are either nonselective, difficult to regenerate, or difficult to produce at large commercial scale.<sup>[1]</sup> Highly efficient, selective, and porous adsorbents developed by low-cost synthesis methods are required to overcome these drawbacks.

Metal-organic frameworks (MOFs) were first reported in the 1950s and the term MOF became popular around the 1990s.<sup>[10,11]</sup> MOFs are crystalline microporous coordination polymers, consisting of metal ions linked together by organic bridging ligands.<sup>[12]</sup> In the past decade, a large variety of MOFs with different topologies and physicochemical properties have been synthesized. Among the most commonly used are MOF-5,<sup>[13]</sup> HKUST-1,<sup>[14]</sup> MIL-47,<sup>[15]</sup> MIL-53,<sup>[16]</sup> the ZIF family,<sup>[17]</sup> MIL-101,<sup>[18]</sup> and UiO-66.<sup>[19]</sup> MOFs exhibit very attractive physicochemical properties such as high porosity (up to 90% free volume), enormous internal surface areas (~1000–10,000 m<sup>2</sup> g<sup>-1</sup>), large pore aperture (~10 nm or 100 Å), and excellent water stability. MOF-based materials have found applications in gas storage and separation,<sup>[20]</sup> sensors,<sup>[21]</sup> catalysis,<sup>[22]</sup> biomass,<sup>[23]</sup> photovoltaic cells,<sup>[24]</sup> drug delivery,<sup>[25]</sup> and environmental remediation.<sup>[26–31]</sup>

In particular, the use of MOF-based materials in wastewater remediation has gained popularity. These coordination polymers can be used either as photocatalysts for organic pollutants degradation<sup>[32,33]</sup> or as adsorbents for the capturing of toxic metals (Hg<sup>II</sup>, Pb<sup>II</sup>, Cr<sup>VI</sup>, U<sup>VI</sup>, etc.).<sup>[34–36]</sup> MOFs can be fabricated on a large scale and with tunable physicochemical properties and functionalities for specific applications. This can be accomplished by changing the synthetic route, metal ions, metal ion sources, and organic linkers. Both organic and inorganic ligands can be employed to tailor the desired MOFs using post-synthesis or in situ

**CONTACT** Nishesh Kumar Gupta  [nishesh0602@gmail.com](mailto:nishesh0602@gmail.com)  283 Goyang-daero, Daehwa-dong, Ilsanseo-gu, Goyang-si, Gyeonggi-do, 10223, Republic of Korea  
Herlys Viltres  [herlysvc.231289@gmail.com](mailto:herlysvc.231289@gmail.com)  Calz Legaria 694, Col. Irrigación, Miguel Hidalgo, 11500 Ciudad de México

approaches. The functionalities anchored onto MOF could be specifically designed to capture specific metal ions, based on their valency. The interaction of electron donors in functional groups with metal ions is governed by the Pearson hard-soft acid-base (HSAB) theory. MOF functionalization with O-ligands like carboxylates are more suitable for complexing tri-valent metal ions like lanthanides and actinides. Whereas S-bearing functionalities (e.g. thiols) are more suitable for capturing divalent heavy metals like  $\text{Hg}^{\text{II}}$  and  $\text{Pb}^{\text{II}}$ . Thus, the fabrication of MOFs with a high density of metal-specific functionalities is efficient for the removal or recovery of metal ions from wastewater, seawater, and ore leachates. The MOF functionalization with desired functional groups is easy as an in-situ or post-synthesis process. Functionalized MOFs can recover target metal ions from poorly concentrated solutions. These qualities have attracted researchers to develop new MOFs with enhanced properties.

In the recent years, literature has been enriched with numerous studies dealing with the recovery of precious metals, lanthanides, and actinides using functionalized MOFs, inducing the need for a compilation in the interest of readers. This is the goal of this review. The first section is dedicated to revisiting some of the most recently used organic moieties as well as the functionalization procedures for tailoring MOFs. Also, relevant physicochemical properties of the functionalized MOFs, including surface area, morphology, and particle size

are reviewed. Sections are dedicated to discussion related to the application of MOFs for heavy metal, precious metal, rare earth elements, and actinides adsorption. Some considerations regarding the advantages and disadvantages of using functionalized MOFs as well as future scope and perspectives are provided.

## Synthesis of functionalized MOFs

MOFs exhibit attractive physicochemical properties, which make these materials suitable for a wide range of applications including water treatment.<sup>[20–22,25,27,28,37]</sup> There are several synthetic approaches to prepare MOFs. They can be classified into conventional and non-conventional methods. Among the conventional methods are hydrothermal<sup>[38]</sup> and solvothermal<sup>[39]</sup> techniques. While the microwave-assisted,<sup>[40]</sup> electrochemical,<sup>[41]</sup> ionothermal,<sup>[42]</sup> and mechanochemical<sup>[43]</sup> strategies are considered as non-conventional approaches. The physical and chemical properties of the prepared MOFs can be tuned to serve a specific application by changing the synthetic route or modifying the components of the framework. For heavy metal remediation, the most common strategy is to anchor organic functionalities (Figure 1) on the easily accessible MOF sites to improve its affinity and selectivity toward the target metal ion. These modifications could be carried out either during the MOF fabrication (in-situ) or after the MOF

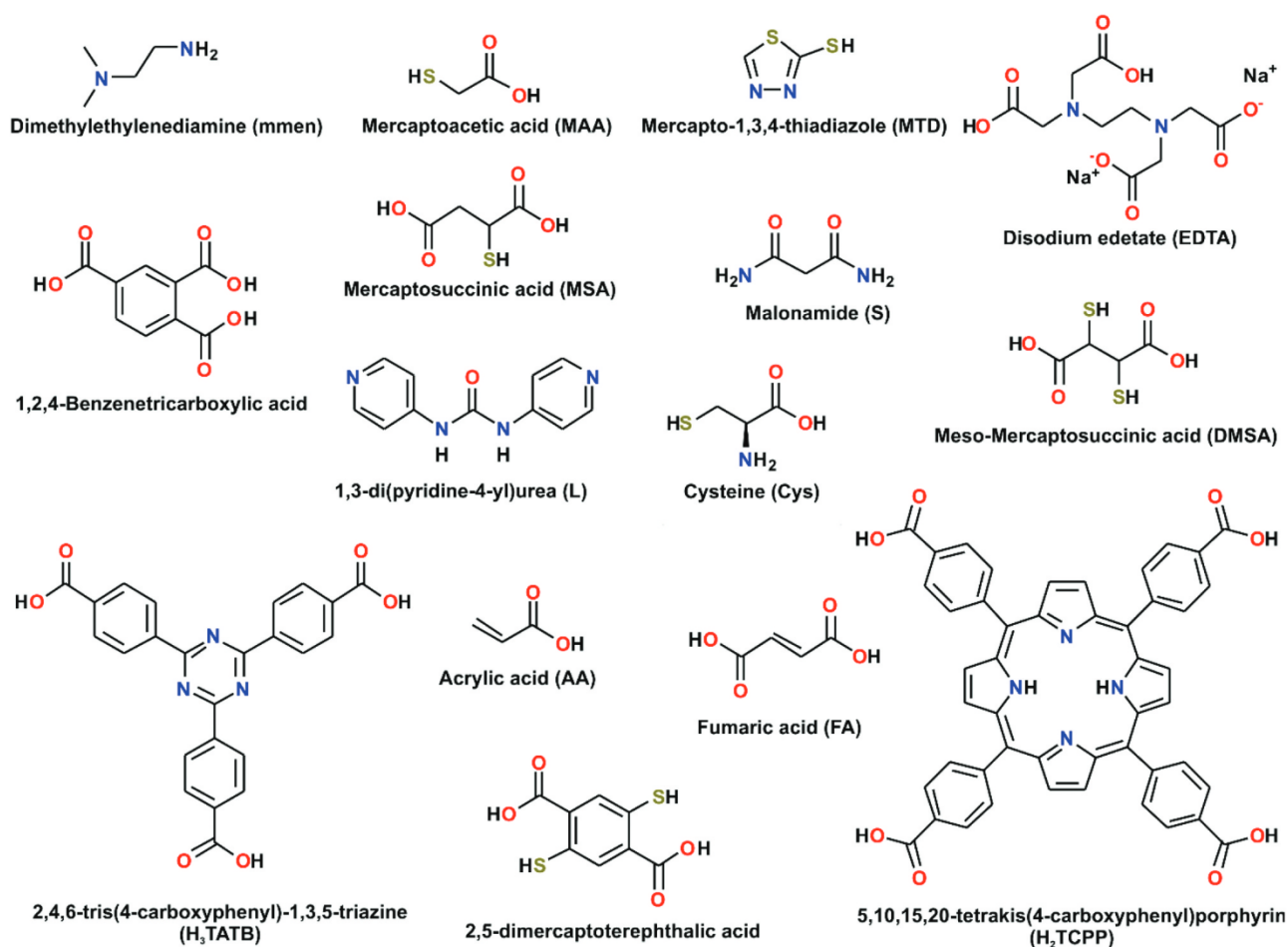


Figure 1. Organic linkers used for the synthesis of functionalized MOFs.

synthesis (post-synthesis). In the subsections, some of the most recent procedures for MOF functionalization using organic ligands are briefly discussed.

### N-based functionalities

Nitrogen-based functionalities (N-donors) are hard to borderline bases in the HSAB theory and could interact effectively with heavy metals and actinides. These N-based organic functionalities have been in focus for decades and incorporating these functionalities into MOFs enhance their affinity toward metal ions. The Zn-based MOF, ZIF-8, grafted with mmen functionality was studied for the adsorptive removal of  $\text{Cd}^{\text{II}}$  from wastewater solutions. ZIF-8 was prepared precipitating  $\text{Zn}(\text{NO}_3)_2 \cdot 6\text{H}_2\text{O}$  and 2-methylimidazole in methanol and adding the mmen diamine in anhydrous hexane and refluxing the suspension for 18 h under  $\text{N}_2$  atmosphere for full MOF functionalization. The decreased intensity of XRD peaks and decreased surface and pores characteristics (estimated by BET analysis) confirmed the grafting of mmen in the pores and the interior surface of ZIF-8.<sup>[44]</sup> A water-stable MOF for  $\text{Pb}^{\text{II}}$  removal was prepared by Zhang et al. through the in-situ modification of a bi-based MOF using a triazine derivative (CAU-7-TATB). The MOF was prepared by a solvothermal method, where 2,4,6-tris(4-carboxyphenyl)-1,3,5-triazine as the organic linker and  $\text{Bi}(\text{NO}_3)_3 \cdot 5\text{H}_2\text{O}$  as the metal source were mixed in a 1:1 v/v DMF-methanol solution. After 0.5 h of stirring, the solution was sealed in a Teflon-lined vial and autoclaved for 44 h at  $130^\circ\text{C}$ . The presence of the donating N in the aromatic ring increased the material affinity toward  $\text{Pb}^{\text{II}}$  ions.<sup>[45]</sup>

Hasankola et al.<sup>[35]</sup> designed a porphyrin modified Zr-MOF (PCN-221) to be used as  $\text{Hg}^{\text{II}}$  sorbent. The PCN-221 MOF was prepared by a solvothermal approach with an in-situ functionalization using 5,10,15,20-tetrakis(4-carboxyphenyl)porphyrin ( $\text{H}_2\text{T CPP}$ ) as the linker. The organic linker was synthesized by dissolving pyrrole and 4-carboxybenzaldehyde in propionic acid and refluxing the mixture for 4 h. After cooling to room temperature, methanol was added and the mixture was cooled in an ice bath leading to the formation of deep-purple crystals of  $\text{H}_2\text{T CPP}$ . The dark red crystals of PCN-

221 were obtained by the solvothermal reaction of  $\text{H}_2\text{T CPP}$ ,  $\text{ZrCl}_4$ , and acetic acid in DMF at  $120^\circ\text{C}$  in a Teflon reactor for 16 h. The similarity between as-synthesized and simulated PXRD patterns of PCN-221 and the appearance of two new peaks around  $1400$  and  $1620\text{ cm}^{-1}$  (corresponding to the coordination of the carboxyl group of the porphyrin ligand to the zirconium metal node) in the FTIR spectrum confirmed the formation of PCN-221.

### O-based functionalities

The oxygen-based functionalities are hard bases that interact strongly with the heavy metals, lanthanides, and actinides in their higher oxidation states. Although the carboxylate functionality is intrinsic to the pristine MOFs synthesized with carboxylate-based organic linkers, grafting specific O-containing functionalities could improve the capacity and selectivity to capture the metal ion of interest. Zhang et al.<sup>[46]</sup> reported the synthesis of carboxyl derivatives of the Zr-based MOF UiO-66 for  $\text{Th}^{\text{IV}}$  capture from acidic solutions. The carboxyl-derivatives UiO-66-COOH were synthesized by heating 1,2,4-benzenetricarboxylic acid,  $\text{ZrCl}_4$ , and water at  $100^\circ\text{C}$  for 24 h in a Teflon-lined autoclave. For UiO-66-(COOH)<sub>2</sub>, 1,2,4,5-benzenetetracarboxylic acid,  $\text{ZrCl}_4$ , and water were refluxed at  $100^\circ\text{C}$  for 24 h. Lou et al.<sup>[47]</sup> developed a series of acrylic acid-functionalized MOFs (y-AA-x@MIL-101s) for the recovery of trivalent rare-earths. The light green MOF crystals were synthesized by blending  $\text{Cr}(\text{NO}_3)_3 \cdot 9\text{H}_2\text{O}$ , terephthalic acid, and glacial acetic acid in water. The above solution with acrylic acid was placed in a Teflon-lined autoclave bomb and placed in an oven at  $200^\circ\text{C}$  for 9 h. Zheng et al.<sup>[34]</sup> prepared MOF-801, a Zr-based MOF with fumaric acid as the linker, for  $\text{Cr}^{\text{VI}}$  adsorption. The MOF was synthesized by the solvothermal reaction between  $\text{ZrOCl}_2 \cdot 8\text{H}_2\text{O}$ , fumaric acid, DMF, and formic acid heated at  $130^\circ\text{C}$  for 6 h in a screw-capped jar.

### S-based functionalities

The use of S-containing MOFs is a common strategy, particularly for the removal of soft-metal ions such as  $\text{Hg}^{\text{I}}$ ,  $\text{Cd}^{\text{II}}$ , and  $\text{Hg}^{\text{II}}$ . The strong interaction between S-donor soft bases and

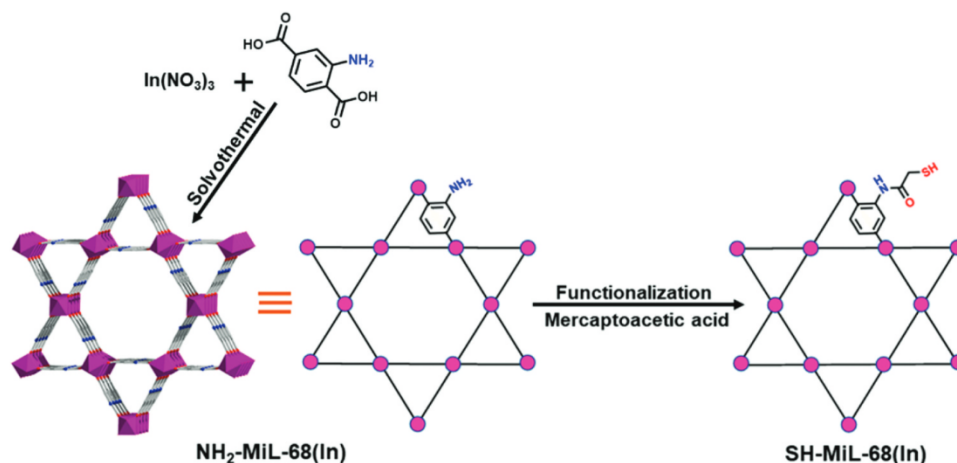


Figure 2. Representation of  $\text{NH}_2\text{-MIL-68(In)}$  post-functionalization using MAA. Reprinted with permission from Ref. 48.<sup>[48]</sup> Copyright (2019) America Chemical Society.

soft acids leads to a favorable adsorption by MOF adsorbents. The post-functionalization of an  $\text{NH}_2\text{-MIL-68(In)}$  MOF with thiol groups was adopted as a novel approach to enhance the MOF selectivity for  $\text{Hg}^{\text{II}}$  uptake from wastewater (Figure 2). The  $\text{NH}_2\text{-MIL-68(In)}$  was prepared by the solvothermal method, where 2-aminoterephthalic acid, benzoic acid, and pyridine were mixed with  $\text{In}(\text{NO}_3)_3$  in DMF and sonicated for 5 min. The mixture was heated at  $125^\circ\text{C}$  in an oven for 2.5 h yielding a light yellow powder. Mercapto acetic acid was added to the synthesized MOF in  $\text{CH}_2\text{Cl}_2$  and kept at room temperature for 12 h, which led to the formation of  $\text{SH-MIL-68(In)}$ . The  $2552\text{ cm}^{-1}$  absorption peaks for the sulfhydryl group,  $\text{C}=\text{O}$   $1634\text{ cm}^{-1}$ ,  $-\text{NH}-$   $1593\text{ cm}^{-1}$ , and  $\text{C}-\text{N}$   $1413\text{ cm}^{-1}$  in the FTIR spectrum confirmed the successful mercaptoacetylation of  $\text{NH}_2\text{-MIL-68(In)}$ . The decrease in the surface area and pore volume after mercaptoacetylation showed a possible occupation of mercapto acetic acid functionalities in the MOF pores.<sup>[48]</sup>

An efficient  $\text{Cr}^{\text{VI}}$  removal was achieved by Yang et al. using two in-situ thiol-modified Zr-MOFs, Zr-MSA and Zr-DMSA, using mercaptosuccinic acid (MSA) and DMSA as organic linkers, respectively (Figure 3). The zirconium precursor and the organic ligand were dissolved in a fumaric acid/water mixture and sonicated for 1 min. Afterward, the mixture was kept in an oven at  $80^\circ\text{C}$  for 2 h for Zr-MSA and at  $95^\circ\text{C}$  for 12 h for Zr-DMSA.<sup>[49]</sup> The prepared MOFs showed very similar PXRD patterns indicating that the two thiol-MOFs had the same crystal structure. Moreover, the presence of thiol functionalities in the Zr-MSA and Zr-DMSA skeletons was confirmed by the appearance of a broad IR band at  $2550\text{ cm}^{-1}$  corresponding to the  $\text{S}-\text{H}$  vibrations.

Recently, Wang et al. reported the selective recovery of  $\text{Au}^{\text{III}}$  using a thiol-MOF,  $\text{UiO-66-MTD}$ . The authors proposed the post-synthetic modification of a  $\text{UiO-66-NH}_2$  using mercapto-1,3,4-thiadiazole, the MTD ligand. First,  $\text{UiO-66-NH}_2$  was prepared by dissolving  $\text{ZrCl}_4$  and 2- $\text{NH}_2$ -benzenedicarboxylate in DMF. The mixture was transferred into a Teflon-lined stainless-steel autoclave and kept in an oven at  $120^\circ\text{C}$  for 48 h. Then,  $\text{UiO-66-NH}_2$  mixed with

glutaraldehyde was reacted at room temperature for 25 h. The precipitate and the MTD ligand were reacted in DMF for 25 h at room temperature leading to the formation of  $\text{UiO-66-MTD}$ . The functionalization procedure was followed by changes in the FTIR spectra of the synthesized materials. The peaks corresponding to the  $\text{N}-\text{H}$  group,  $1662$ ,  $3338$ , and  $3467\text{ cm}^{-1}$  disappeared after the glutaraldehyde modification. Instead, two new peaks at  $1499$  and  $1683\text{ cm}^{-1}$  attributed to  $\text{C}=\text{N}$  and  $\text{C}=\text{O}$  vibrations, appeared. The incorporation of thiol functionality was confirmed with the disappearance of the  $1683\text{ cm}^{-1}$  peak and the appearance of a new one at  $2495\text{ cm}^{-1}$  for  $-\text{SH}$  vibrations.<sup>[50]</sup>

A thiol functionalized MOF,  $\text{UiO-66-(SH)}_2$ , was used as a porous matrix for  $\text{CeO}_2$  nanoparticle encapsulation. The  $\text{CeO}_2@\text{UiO-66}$  was prepared by the spray-drying method and was tested for single and multi-metal adsorption of  $\text{As}^{\text{III}}$ ,  $\text{As}^{\text{V}}$ ,  $\text{Cd}^{\text{II}}$ ,  $\text{Cr}^{\text{III}}$ ,  $\text{Cr}^{\text{VI}}$ ,  $\text{Cu}^{\text{II}}$ ,  $\text{Pb}^{\text{II}}$ , and  $\text{Hg}^{\text{II}}$ . In a flask containing DMF, terephthalic acid, glacial acetic acid,  $\text{CeO}_2$  nanoparticles, and  $\text{Zr}^{\text{IV}}$  propoxide ( $\text{Zr(OPr)}_4$ ) were added. The mixture was transferred into a 3 mm coil-flow reactor at  $115^\circ\text{C}$  with a feed rate of  $2.4\text{ mL min}^{-1}$ . Finally, the solution was spray-dried at  $180^\circ\text{C}$  and a flow rate of  $336\text{ mL min}^{-1}$ . The obtained  $\text{CeO}_2@\text{UiO-66}$  was dispersed in DMF, washed with DMF/ethanol, and dried at  $85^\circ\text{C}$  for 12 h. The thiol modified material,  $\text{CeO}_2@\text{UiO-66-(SH)}_2$ , was prepared by following the described procedure but replacing terephthalic acid by 2,5-dimercaptoterephthalic acid. The  $\text{CeO}_2$  nanoparticles encapsulation efficiency estimated by ICP-AES confirmed 93% and 87% encapsulation yields for the  $\text{CeO}_2@\text{UiO-66}$  and  $\text{CeO}_2@\text{UiO-66-(SH)}_2$ , respectively. The encapsulation of  $\text{CeO}_2$  nanoparticles was also confirmed by high-angle annular dark-field scanning transmission electron microscopy images showing the presence of  $\text{CeO}_2$  nanoparticles inside the MOF beads.<sup>[51]</sup>

### Mixed functionalities

The synthesis of MOFs containing mixed functionalities like  $-\text{SH}$ ,  $-\text{NH}_2$ , or  $-\text{COOH}$  groups is another strategy adopted to

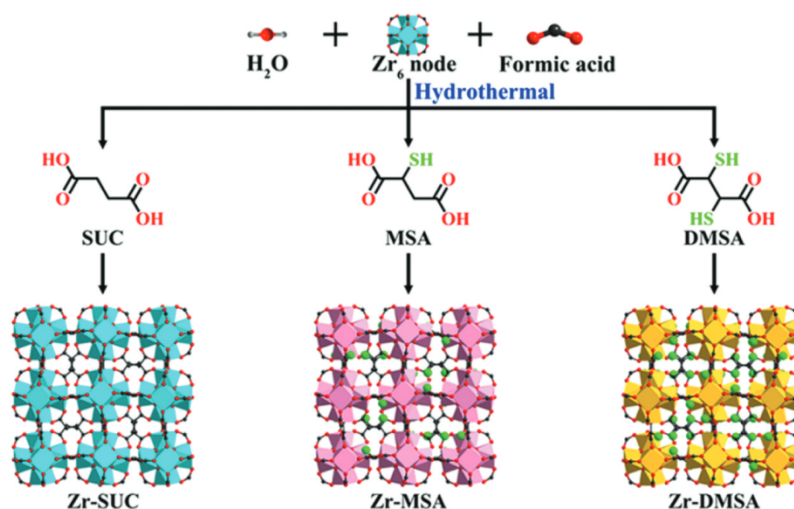


**Figure 3.** Representation of in-situ functionalization of Zr-MOFs using succinic acid (SUC), and the mercapto MSA and DMSA. Adapted with permission from Ref. 49.<sup>[49]</sup> Copyright (2019) America Chemical Society.

capture both hard and soft metal ions from waste solutions containing a matrix of contaminants. An EDTA functionalized MOF was prepared to be used as an adsorbent for  $\text{Hg}^{\text{II}}$  and  $\text{Pb}^{\text{II}}$ . Firstly, the UiO-66 MOF was synthesized by a solvothermal method, where  $\text{ZrCl}_4 \cdot 8\text{H}_2\text{O}$  and terephthalic acid were prepared in DMF separately and mixed under stirring with acetic acid. The final solution was transferred into a Teflon-lined stainless-steel autoclave and heated for 18 h at  $90^\circ\text{C}$ . The white solid, UiO-66, was washed using DMF and activated in methanol. Afterward, the activated solid was dispersed in deionized water and EDTA disodium salt was added. The reaction mixture was stirred and heated at  $60^\circ\text{C}$  for 24 h leading to UiO-66-EDTA. The introduction of EDTA into the modified MOF pores was confirmed by a 64% and 62% decrease in the surface area and pore volume, respectively. Moreover, a noticeable shift in the Zr 3d HRXPS spectrum after the EDTA introduction confirmed the formation of UiO-66-EDTA. The authors suggested that the shift could be due to the replacement of carboxyl groups of the pristine UiO-66 by EDTA in UiO-66-EDTA, being the COOH groups of EDTA the ones coordinated with  $\text{Zr}_6$ , indicating that the hexadentate ligand is chemically grafted into the MOF.<sup>[52]</sup>

A dual in-situ functionalization of a Zn-based MOF, TMU-32S, using 1,3-di(pyridine-4-yl)urea and malonamide ligand (S) was proposed as a novel  $\text{Hg}^{\text{II}}$  adsorbent. The TMU-32 precursor was prepared by mixing the organic ligands 4,4'-oxydibenzoic acid and 1,3-di(pyridine-4-yl)urea with  $\text{Zn}(\text{NO}_3)_2$  for 72 h at  $100^\circ\text{C}$ . Later, the malonamide ligand was dissolved and sonicated for 5 min. The white TMU-32 MOF crystals were soaked in the ligand solution and dried at  $80^\circ\text{C}$ . The incorporation of S ligand in the MOF led to a color change from white to light brown. In the  $^1\text{H}$  NMR spectrum, the two doublet signals (7.96 and 8.73 ppm) were associated with the urea ligand while the signals at 3.53, 7.85, and 7.66 ppm, were related to the malonamide linker. The analysis of the signal intensity after 3, 6, and 10 days suggested that 33%, 65%, and 100% of urea were replaced by S ligands, respectively.<sup>[53]</sup> An L-cysteine modified UiO-66 was proposed as a novel adsorbent for  $\text{Hg}^{\text{II}}$  removal from water. The  $\text{NH}_2$ -UiO-66 precursor was prepared by mixing  $\text{ZrCl}_4$ , 2-aminoterephthalic acid, and HCl at  $130^\circ\text{C}$  for 24 h. In the first modification step, the precursor and 1,4-phthalaldehyde were mixed in DMF at  $70^\circ\text{C}$  for 24 h. The obtained solid, PA-UiO-66, was washed and dried. The final modification was performed by mixing PA-UiO-66, L-cysteine, and DMF and heating it for 24 h at  $70^\circ\text{C}$  to form Cys-UiO-66. The appearance of a band at  $2559\text{ cm}^{-1}$  corresponding to the S – H group in the FTIR spectrum, confirmed the grafting of the L-cysteine onto PA-UiO-66.<sup>[54]</sup>

### Physicochemical properties of MOFs

The adsorption process can be understood as the adhesion of an adsorbate, i.e. atoms, ions, or molecules, from a gas, liquid, or dissolved solid to a solid surface creating a film on the adsorbent surface. Since it is a phenomenon that occurs on the surface, adsorbents with the higher surface area will favor the adsorption process. In that sense, MOF-based adsorbents have gained a lot of attention due to their high surface area

estimated by using  $\text{N}_2$  adsorption-desorption isotherm with Brunauer–Emmett–Teller (BET) equation.<sup>[55]</sup> The surface area of a MOF primarily depends on the metal ion and organic linker and to some extent is controlled by the synthesis route, solvent, etc. The modification of MOFs with organic functionalities leads to the grafting of these functionalities into the MOF pores, which decreases the surface area and pore diameter. Briefly, the adsorption process on the MOF occurs due to the presence of numerous active sites on the surface and by diffusion of metal ions through the pores of the framework. The decrease in the surface area is overcompensated by the presence of numerous active sites on the surface for the binding of metal ions. The pores of MOFs are highly ordered due to their crystalline structure and pore size distribution. Using the Barrett, Joyner, and Halenda method,<sup>[55]</sup> the MOF pore diameters are within the 0.5–5.0 nm range. Another important aspect is related to the compatibility between pore size and the ionic radius of the adsorbate to ensure high sorption capacities. Since the ionic diameter of metal ions is much smaller than the MOF pore diameters, the diffusion process remains unhindered. Table 1 summarizes the physical and structural properties of differently functionalized MOFs.

A key prerequisite for an adsorbent to be applied for wastewater treatment is its water stability. Wastewaters of industrial origin have a wide pH range, which largely depends on the constituents. The high-level waste solutions originating from nuclear energy facilities are highly acidic. A common method to assess the water stability of the MOF is to soak it in solutions of different pHs for a long time and comparing the XRD patterns before and after soaking. If no variations are observed in diffraction peaks intensity and Bragg positions after the material exposure to pH variations, the MOF is expected to show good water stability. Zr-MOFs are one of the most widely used for heavy metal decontamination due to their high structural stability in basic/acidic media.<sup>[70–72]</sup> Studies dealing with the recovery of actinides from seawater lack such pH evaluations, which make it difficult to comment on their capability in the field of nuclear waste management.

The presence of specific moieties on the MOF surface creates recognition sites, which leads to selective host-guest interactions. In the past few years, the tailoring of MOFs with task-specific organic functionalities has become a common strategy for the capturing of specific metal ions from a matrix. The most used functionalities are those containing amine, thiol, carboxylate, and hydroxyl groups. The ligands containing O, N, and S as the donors could be classified as hard, hard to borderline and soft bases, respectively, according to Pearson HSAB theory. Thus, soft and borderline metal ions such as  $\text{Hg}^{\text{II}}$ ,  $\text{Hg}^{\text{I}}$ ,  $\text{Pb}^{\text{II}}$ ,  $\text{Pd}^{\text{II}}$ ,  $\text{Cd}^{\text{II}}$ ,  $\text{Ag}^{\text{I}}$ , and  $\text{Au}^{\text{III}}$  can be more efficiently adsorbed by modified MOF containing either N or S-donors. Likewise, MOFs with O-donor functionalities exhibit a higher binding affinity for hard metal ions such as  $\text{Cr}^{\text{III}}$ ,  $\text{As}^{\text{III}}$ ,  $\text{Ln}^{\text{III}}$ ,  $\text{Th}^{\text{IV}}$ , and  $\text{U}^{\text{VI}}$ .<sup>[46,66,73,74]</sup> The newest approach of using macrocyclic groups or chelating ligands with multiple donating sites have shifted the attention toward designing highly selective metal-binding ligands and their anchoring on the MOF surface.<sup>[35]</sup>

**Table 1.** Physical properties of functionalized-MOF.

MOF	Physical properties				
	$S_{\text{BET}}$ ( $\text{m}^2 \text{g}^{-1}$ )	$D_p$ (nm)	Morphology	Particle size (nm)	Ref
ZIF-8-mmen	970	1.5	Circular	50	[44]
CAU-7-TATB	220	2.6	Flat	800	[45]
$\text{NH}_2\text{-SiO}_2\text{@Cu-MOF}$	1100	-	Octahedral	-	[56]
PCN-221	-	-	Spherical	-	[35]
MIL-101(Cr)- $\text{NH}_2$	1450	-	Prismatic	150	[36]
UiO-66-PEIs	420	2.5	Cubic	-	[57]
TMU-23	-	-	Sheet	-	[58]
$\text{NH}_2\text{-ZIF-8}$	1250	-	-	-	[59]
UiO-66-(COOH) $_2$	130	-	-	174	[47]
MOF-801	735	-	Octahedral	1500	[34]
UiO-66-(COOH) $_2$	440	-	-	-	[60]
SH-MIL-68(In)	290	0.6	-	-	[48]
Zr-MOFs-SH	-	1.9	Cubic	1400	[61]
MMPF-6-SH	750	-	Needlelike	-	[62]
MIL-101-SH	1540	-	-	-	[63]
UiO-66-SH	460	-	-	-	
Zr-MSA	510	-	-	40	[49]
Zr-DMSA	275	-	-	25	
UiO-66-ATU	340	3.8	Irregular disc	-	[64]
$\text{CeO}_2\text{@UiO-66-(SH)}_2$	540	-	Spherical	1500	[51]
UiO-66-MTD	460	1.0	Octahedral	-	[50]
UiO-66-TA	500	-	Octahedral	-	[65]
EDTA-chitosan/Cu-BTC	35	2.7	Octahedral	-	[66]
UiO-66-EDTA	380	-	Octahedral	500	[52]
UiO-66-X	800	3.0	-	-	[67]
TMU-32S-65%	560	-	-	-	[53]
UiO-66-RSA	930	-	Octahedral	-	[68]
MIL-101-OA	2920	-	-	3000	[69]
MIL-101-triglycine	1070	3.4	Spherical	-	[70]
Cys-UiO-66	570	3.8	-	-	[54]
UiO-66-ATA(Zr)	575	1.0	Octahedral	-	[71]
MOFs-DHAQ	160	-	Polygonal	-	[72]

$S_{\text{BET}}$ : Surface area determines by the BET method.  $D_p$ : Average pore diameter calculated by the BJH method.

## Functionalized MOFs for metal adsorption

There are a great variety of methods reported in the literature for metal ions removal, such as coagulation/precipitation, filtration, membranes, biological process, and adsorption among others. The adsorption-based methods are the most commonly used given their simplicity, relatively low cost if the adsorbent is reusable. A concise overview of the application of functionalized MOFs as potential adsorbents for the capturing of metal ions is presented in subsequent subsections. The possible adsorption mechanisms are discussed to help readers to have a better understanding of sorbent-sorbate interactions. Table 2 summarizes the adsorption capacity of functionalized MOFs for metal ions and radionuclides from contaminated water. The adsorption capacity of different adsorbents reported in the literature for heavy metals and actinides have been summarized in Table 3. This detailed literature review suggests that functionalized MOFs have remarkable adsorption capacities for the removal and recovery of metal ions.

## MOFs for heavy metals

Contamination of waterbodies by heavy metal ions has serious consequences on human health and environment.<sup>[35,54,115]</sup> The cellular toxicity arising from the presence of heavy metals in the living systems has been amplified by the inability of the body to discharge them out of the system.<sup>[115]</sup> Modernization induces more heavy metal contamination of waterbodies. Thus, there is a need for severe intervention from the governments,

international bodies, environmentalists, and policymakers. The task to develop diverse remediation methodologies must be taken by researchers. They already explored numerous techniques, such as electrocoagulation,<sup>[116]</sup> chemical precipitation,<sup>[117]</sup> ultra-filtration,<sup>[118]</sup> solvent extraction,<sup>[119]</sup> photocatalysis,<sup>[120]</sup> reverse osmosis, nano-filtration,<sup>[121]</sup> oxidation/reduction,<sup>[122]</sup> and biological treatments<sup>[123]</sup> for heavy metal removal from wastewater. However, some of these processes have limitations due to the high capital investment required for the development and management of the technologies, which may or may not be suitable for underdeveloped countries. Adsorption is considered as an affordable method, which is actively used in several wastewater treatment facilities across the globe with activated carbon as the commercial adsorbent for the removal of impurities in various stages of the treatment process. Among different porous adsorbents, heavy metal capture using functionalized MOFs may come useful in the coming decades. Functionalized MOFs employing different functional groups ( $-\text{NH}_2$ ,  $-\text{SH}$ ,  $-\text{OH}$ , and  $-\text{COOH}$ ) for wastewater remediation is in its developing stage as is discussed scanning the recent published reports.

## MOFs for lead removal

The increasing concentration of Pb in freshwater bodies arising from the liquid discharge of petrochemical industries, smelters, paint and pigment industries, battery manufacturing, and recycling units have raised serious concerns for safe and healthy well-being. It is one of the most toxic metals, which affects almost every organ in the body. Among all the organs, the nervous system is the most affected by  $\text{Pb}^{\text{II}}$  poisoning, which is

MOF	Metal ion	Experimental conditions				$q_m$ (mg g <sup>-1</sup> )	Mechanism	Cycles (% efficiency)	Ref
		C <sub>0</sub> (ppm)	pH	Time (h)	T (°C)				
DUT-67	Pb <sup>II</sup>	100	5.0	24.0	25	98.5	Complexation	5 (-)	[75]
MOFs-DHAQ	Pb <sup>II</sup>	100	4.0	0.5	25	213.3	Complexation	4 (83)	[72]
NH <sub>2</sub> -SiO <sub>2</sub> @Cu-MOF	Pb <sup>II</sup>	50	6.0	0.5	25	166.7	Complexation	7 (80)	[56]
Fe <sub>3</sub> O <sub>4</sub> -NHSO <sub>3</sub> H@HKUST-1	Pb <sup>II</sup>	5	7.0	4.0	25	384.6	Complexation	4 (90)	[76]
UiO-66-ATA(Zr)	Pb <sup>II</sup>	100	5.0	2.0	25	387.0	Chelation, ion Exchange	8 (90)	[71]
TMU-23	Pb <sup>II</sup>	125	7.0	0.5	25	434.7	Complexation	3 (75)	[58]
CAU-7-TATB	Pb <sup>II</sup>	50	7.0	24.0	25	50.6	Complexation	- (-)	[45]
UiO-66-(COOH) <sub>2</sub>	Pb <sup>II</sup>	500	5.0	24.0	25	420.2	Coordination	- (-)	[60]
ZIF-8-mmen	Cd <sup>II</sup>	50	2.0	1.5	25	1000.0	-	- (-)	[44]
HS-mSi@MOF-5	Cd <sup>II</sup>	-	6.0	5.0	10	312.5	Electrostatic interaction, complexation	- (-)	[77]
SH-MIL-68(In)	Hg <sup>II</sup>	10	4.0	12.0	25	450.0	Complexation	5 (100)	[48]
TMU-32S-65%	Hg <sup>II</sup>	100	4.4	0.3	25	1428.0	Complexation	5 (60)	[53]
PCN-221	Hg <sup>II</sup>	120	7.1	0.5	25	233.0	-	3 (80)	[35]
MIL-101-SH	Hg <sup>II</sup>	100	5.0	2.0	25	250.0	Complexation	5 (80)	[63]
UiO-66-SH						110.0		5 (90)	
Cys-UiO-66	Hg <sup>II</sup>	100	5.0	3.0	30	350.1	Chelation	5 (80)	[54]
Zr-MSA	Hg <sup>II</sup>	10	7.0	0.1	25	734.0	Complexation	5 (96)	[78]
Zr-MSA	Cr <sup>VI</sup>	30	3.0	24.0	25	202.0	Reduction-complexation	- (-) (-)	[49]
Zr-DMSA						138.7			
Fe <sub>3</sub> O <sub>4</sub> @UiO-66@UiO67/CTAB	Cr <sup>VI</sup>	50	2.0	24.0	25	932.1	Electrostatic interactions	5 (92)	[79]
EDTA-chitosan/Cu-BTC	Cr <sup>VI</sup>	20	2.0	2.0	25	46.5	Electrostatic interactions	5 (100)	[66]
MOF-801	Cr <sup>VI</sup>	50	7.0	1.0	25	156.2	Electrostatic interactions	4 (89)	[34]
UiO-66(NH <sub>2</sub> )	As <sup>III</sup>	100	9.2	-	25	200.0	Complexation	6 (87)	[80]
	As <sup>V</sup>					71.1		6 (83)	
UiO-66(NH <sub>2</sub> )	Sb <sup>III</sup>	500	4.3	2.0	25	61.8	Electrostatic interaction, coordination	- (-) (-)	[81]
	Sb <sup>V</sup>					105.4			
Fe <sub>3</sub> O <sub>4</sub> @TA@UiO-66	As <sup>III</sup>	40	3.0	24.0	25	97.8	Complexation, hydrogen bonding	- (-) (-)	[82]
	Sb <sup>III</sup>					50.3			
MMPF-6-SH	Cu <sup>II</sup>	400	5.0	-	25	42.7	-	30 (86)	[62]
UiO-66-PEIs	Cu <sup>II</sup>	40	6.0	1.0	25	24.9	-	4 (90)-(-)	[57]
	Ni <sup>II</sup>					11.5			
MIL-101(Cr)-NH <sub>2</sub>	Pd <sup>II</sup>	100	1.0	24.0	25	127.3	Electrostatic interactions	5 (100)	[36]
	Pt <sup>IV</sup>					35.1		5 (100)	
UiO-66-COOCH <sub>3</sub>	Co <sup>II</sup>	10	8.4	24.0	25	334.4	Chelation	5 (95)	[67]
UiO-66-COONH <sub>2</sub>						339.7		5 (95)	
UiO-66-CN						274.6		5 (95)	
UiO-66-SO <sub>3</sub> H						293.7		5 (95)	
MIL-101-triglycine	Co <sup>II</sup>	10	8.3	36.0	25	232.6	Coordination	- (-)	[70]
UiO-66-MTD	Au <sup>III</sup>	100	6.0	3.0	25	310.5	Ion exchange, chelation	3 (87)	[50]
UiO-66-TA	Au <sup>III</sup>	100	2.0	20.0	25	374.0	Chelation, ion exchange	6 (90)	[65]
ZT-MOF	Au <sup>III</sup>	200	-	24.0	25	333.3	Coordination	4 (88)	[83]
NH <sub>2</sub> -ZIF-8	Au <sup>III</sup>	150	3.3	1.5	25	375.0	Electrostatic interaction	3 (95)	[59]
	Ag <sup>I</sup>					22.2		3 (95)	
Magnetite@MIL-101-SO <sub>3</sub>	Y <sup>III</sup>	-	4.5	0.1	25	15.0	Complexation	- (-) (-) (-) (-) (-) (-) (-) (-) (-)	[84]
Magnetite@DETA-In-MOF	Ce <sup>III</sup>					33.0			

(Continued)

Table 2. (Continued).

MOF	Metal ion	Experimental conditions				$q_m$ (mg g <sup>-1</sup> )	Mechanism	Cycles (% efficiency)	Ref
		C <sub>0</sub> (ppm)	pH	Time (h)	T (°C)				
HKUST-1	Ce <sup>III</sup>	-	6.0	8.0	25	353.0	Complexation, ion-exchange	3 (10)	[86]
UiO-66-EDTA	Eu <sup>III</sup>	80	5.0	10.0	30	195.2	Complexation	6 (90)	[52]
	Hg <sup>II</sup>					371.6		6 (90)	
	Pb <sup>II</sup>					356.9		6 (90)	
MIL-125-HQ	Pb <sup>II</sup>	500	7.0	-	25	262.1	Complexation	4 (78)	[87]
	Cd <sup>II</sup>					102.8		4 (73)	
	Cu <sup>II</sup>					66.9		4 (74)	
	Cr <sup>III</sup>					53.9		4 (75)	
Azo-MOF	U <sup>VI</sup>	100	2.0	5.0	25	200.0	Complexation	- (-)	[88]
ECUT-100	U <sup>VI</sup>	300	2.0	5.7	25	381.0	Complexation	- (-)	[89]
MIL-101-OA	U <sup>VI</sup>	10	8.0	1.0	25	321.0	-	6 (92)	[69]
MIL-53(Al)-AO	U <sup>VI</sup>	100	6.0	8.3	25	137.0	-	5 (85)-(-)	[90]
MIL-53(Al)-NH <sub>2</sub>						54.0			
HKUST-1	U <sup>VI</sup>	200	6.0	2.0	25	332.0	Complexation, electrostatic interaction	- (-)	[91]
Co-SLUG-35	U <sup>VI</sup>	100	-	4.0	25	118.0	Anion-exchange	3 (50)	[92]
DSHM-DAMN	U <sup>VI</sup>	400	8.0	4.0	25	601.0	Complexation	5 (95)	[93]
MOF-5	U <sup>VI</sup>	300	0.1	24.0	25	237.0	Complexation, electrostatic interaction	- (-)	[94]
MIL-101-COOH	U <sup>VI</sup>	50	7.0	2.0	25	314.0	Electrostatic interaction	3 (50)	[74]
MIL-101-NH <sub>2</sub>	U <sup>VI</sup>	100	5.5	4.0	25	95.0	Complexation	- (-)- (-)- (-)	[95]
MIL-101-ED						229.0			
MIL-101-DETA						410.0			
Zn(HBTC)(L)(H <sub>2</sub> O) <sub>2</sub>	U <sup>VI</sup>	100	2.0	-	25	126.0	Complexation	- (-)	[96]
UiO-68-2	U <sup>VI</sup>	100	2.5	1.0	23	217.0	-	- (-)- (-)	[97]
UiO-68-3						109.0			
Fe <sub>3</sub> O <sub>4</sub> @AMCA-MIL53(Al)	U <sup>VI</sup>	20	-	24.0	25	227.0	Complexation, electrostatic interaction	- (-)- (-)	[98]
	Th <sup>IV</sup>					286.0			
MIL-100(Al)	U <sup>VI</sup>	-	3.0	0.3	25	110.0	-	- (-)- (-)	[99]
	Th <sup>IV</sup>					167.0			
UiO-66	Th <sup>IV</sup>	100	3.0	6.0	25	13.0	Complexation, electrostatic interaction	2 (50)	[46]
UiO-66-COOH						118.0		2 (50)	
UiO-66-(COOH) <sub>2</sub>						370.0		2 (50)	
Ho-MOF	Th <sup>IV</sup>	0.1	5.0	-	25	350.0	Complexation	- (-)	[73]

Table 3. Summary of adsorbents employed for the removal of heavy metals and actinides.

MOF	Metal ion	Experimental conditions				$q_m$ (mg g <sup>-1</sup> )	Remarks	Ref
		C <sub>0</sub> (ppm)	pH	Time (h)	T (°C)			
Graphene Nanosheets	Pb <sup>II</sup>	40	4	15	30	35.7	Low adsorption capacity with no reusability study	[100]
GO	Cu <sup>II</sup>	20	0	-	30	72.6	Excellent reusability but desorption at pH 0	[101]
	Cd <sup>II</sup>					83.6		
	Ni <sup>II</sup>					62.3		
Oxidized MWCNTs	Cu <sup>II</sup>	30	5	4	30	28.4	High production cost	[102]
	Cd <sup>II</sup>					10.9		
	Pb <sup>II</sup>					97.1		
Groundnut husk AC	Cr <sup>VI</sup>	-	2	7	25	131.0	High adsorption at pH 2	[103]
Cotton stalk AC	Pb <sup>II</sup>	100	4.4	48	25	70.3	No reusability study	[104]
MoS <sub>4</sub> <sup>2-</sup> intercalated Mg-Al-NO <sub>3</sub> -LDH	Cu <sup>II</sup>	30	-	24	25	181.0	High adsorption capacity but no reusability study	[105]
	Pb <sup>II</sup>					290.0		
	Hg <sup>II</sup>					500.0		
Conjugated microporous polymer-2	Pb <sup>II</sup>	10	-	12	25	62.7	Poor desorption efficiency	[106]
Conjugated microporous polymer-3						93.2		
Thiol Grafted Imine-Based Covalent Organic Framework	Hg <sup>II</sup>	10	5.6	2	25	4395.0	Exceptional adsorption capacity with selectivity but no reusability study	[107]
SiO <sub>2</sub> encapsulated natural zeolite	Pb <sup>II</sup>	10	-	1	25	186.0	Good reusability but low adsorption capacity	[108]
	Cd <sup>II</sup>					10.3		
	Cu <sup>II</sup>					12.3		
Dihexyl amide-functionalized MWCNT	Th <sup>IV</sup>	10	4	48	20	47.0	Good radiolytic stability but low adsorption capacity	[109]
	U <sup>VI</sup>					32.0		
GO in calcium alginate	U <sup>VI</sup>	10	6	2	25	29.4	Slow kinetics with low adsorption capacity	[110]
Amidoxime zeolite	U <sup>VI</sup>	200	4.5	2	10	5.0	Possible radiolytic stability but low adsorption capacity	[111]
Phosphonic functional groups mesoporous SiO <sub>2</sub>	U <sup>VI</sup>	14.3	2.8	-	25	207.6	Good adsorption capacity but with low selectivity	[112]
Magnetic talc TiO <sub>2</sub> composite	Th <sup>IV</sup>	250	4	2	25	54.5	Good desorption efficiency but no selectivity study	[113]
Wrinkled mesoporous carbon	Th <sup>IV</sup>	0.3	2.2	4	25	8.7	Excellent selectivity in the presence of lanthanides with low adsorption capacity	[114]

GO: graphene oxide; AC: activated carbon; LDH: layered double hydroxide.

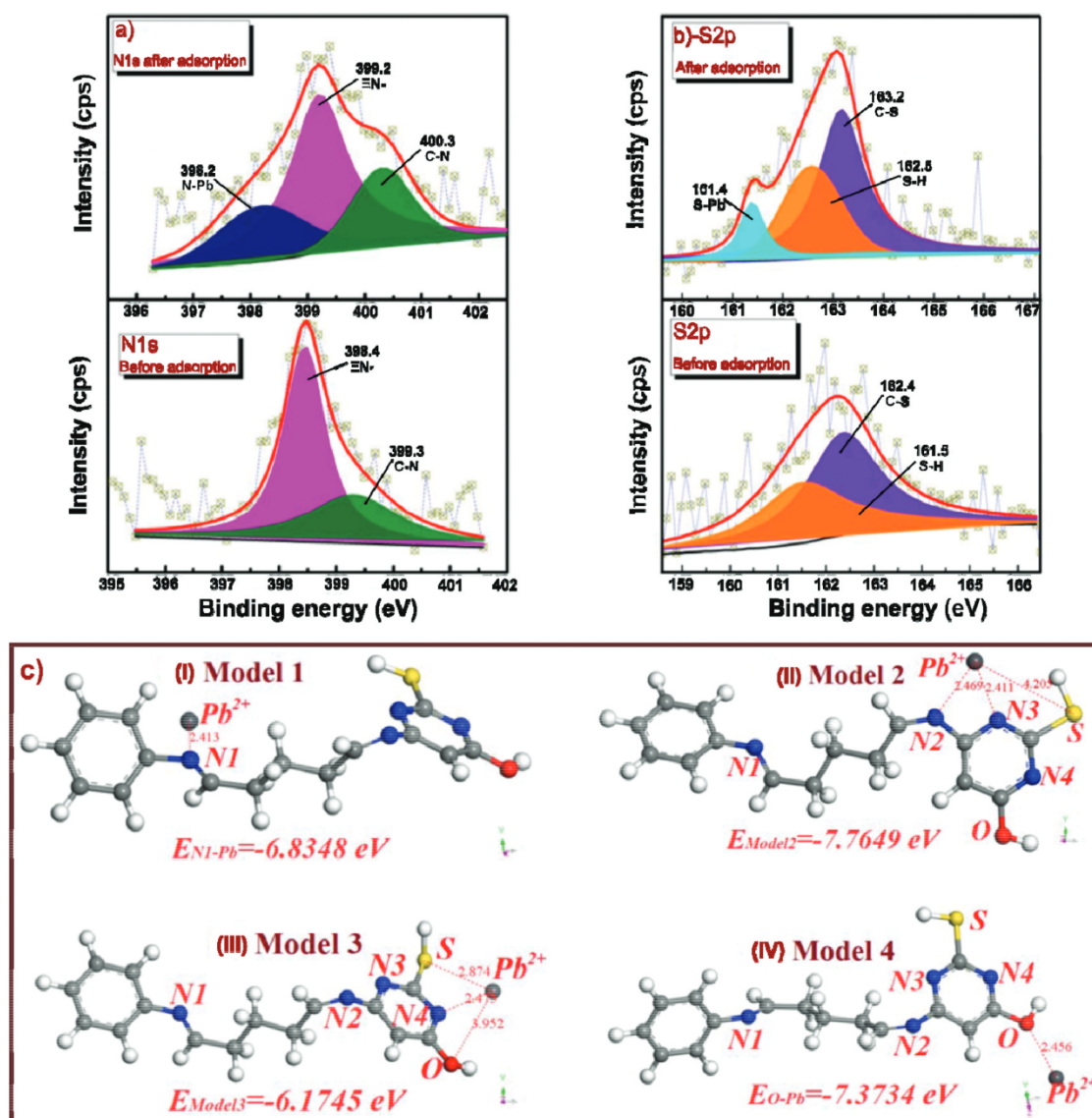


**Figure 4.** (a) High-resolution spectra of N 1s; (b) S 2p before and after Pb<sup>II</sup> adsorptive removal employing UiO-66-amino thiouracil (ATA)(Zr); (c) the optimized geometries, binding energies and bond lengths of UiO-66-ATA(Zr) adsorbing lead at different single ligand binding sites. The black, white, blue, red, yellow, and dark gray spheres correspond respectively to carbon, hydrogen, nitrogen, oxygen, sulfur, and lead atoms.

much more serious for children than adults.<sup>[124]</sup> Thus, it is necessary to explore efficient adsorbent for the trapping of Pb<sup>II</sup> from wastewater. In the literature, the application of functionalized MOFs for the sequestration of Pb<sup>II</sup> ions has been reported on many occasions. Zhao et al.<sup>[72]</sup> developed a dihydroxyanthraquinone (DHAQ) functionalized MOF for the remediation of Pb-enriched wastewater. The XPS analysis of the MOF-DHAQ-Pb confirmed a strong complexation of Pb<sup>II</sup> ions through the DHAQ hydroxyl and carbonyl functionalities. Another binding possibility was the monodentate Pb<sup>2+</sup> binding with N-atoms of the DHAQ linkage. These binding modes were systematically validated by the energy calculations using the DFT theory.

The broad breakthrough curve in the column study was the limiting factor for the practicality of the MOF-DHAQs for the treatment of industrial wastewater. The possible coordination of Pb<sup>II</sup> ions with amine functionalities was reported over NH<sub>2</sub>-SiO<sub>2</sub>@Cu-MOF, where the maximum adsorption capacity of

167 mg g<sup>-1</sup> was reported. The adsorbent was applied to the water of the Karoon River, Iran, spiked with 5–50 mg L<sup>-1</sup> of Pb<sup>II</sup> ions. The adsorbent was able to remove ~95% of Pb<sup>II</sup> ions at 5 mg L<sup>-1</sup> Pb<sup>2+</sup> concentration, which decreased to ~82% for 50 mg L<sup>-1</sup>.<sup>[56]</sup> Selective and efficient adsorption of Pb<sup>II</sup> ions with ATA functionality anchored on UiO-66 was reported by Xiong et al.,<sup>[71]</sup> where the adsorption capacity reached to 387 mg g<sup>-1</sup> at pH 4. The shift in the binding energy of O-, N-, and S-sites of UiO-66-ATA(Zr) in their respective HRXPS spectrum and appearance of new peaks for Pb–O (530.8 eV), Pb–N (398.2 eV), and Pb–S (161.4 eV) suggested the involvement of amino, sulfhydryl, and hydroxyl groups in the adsorption process via chelation, ion exchange, and electrostatic interactions (Figures 4a and b). The DFT calculations were done for different binding modes of Pb<sup>2+</sup> with the N/S/O binding sites of the UiO-66-ATA(Zr) adsorbent (Figure 4c). Based on the energy and bond length considerations in different optimized geometries, it was concluded that the interaction

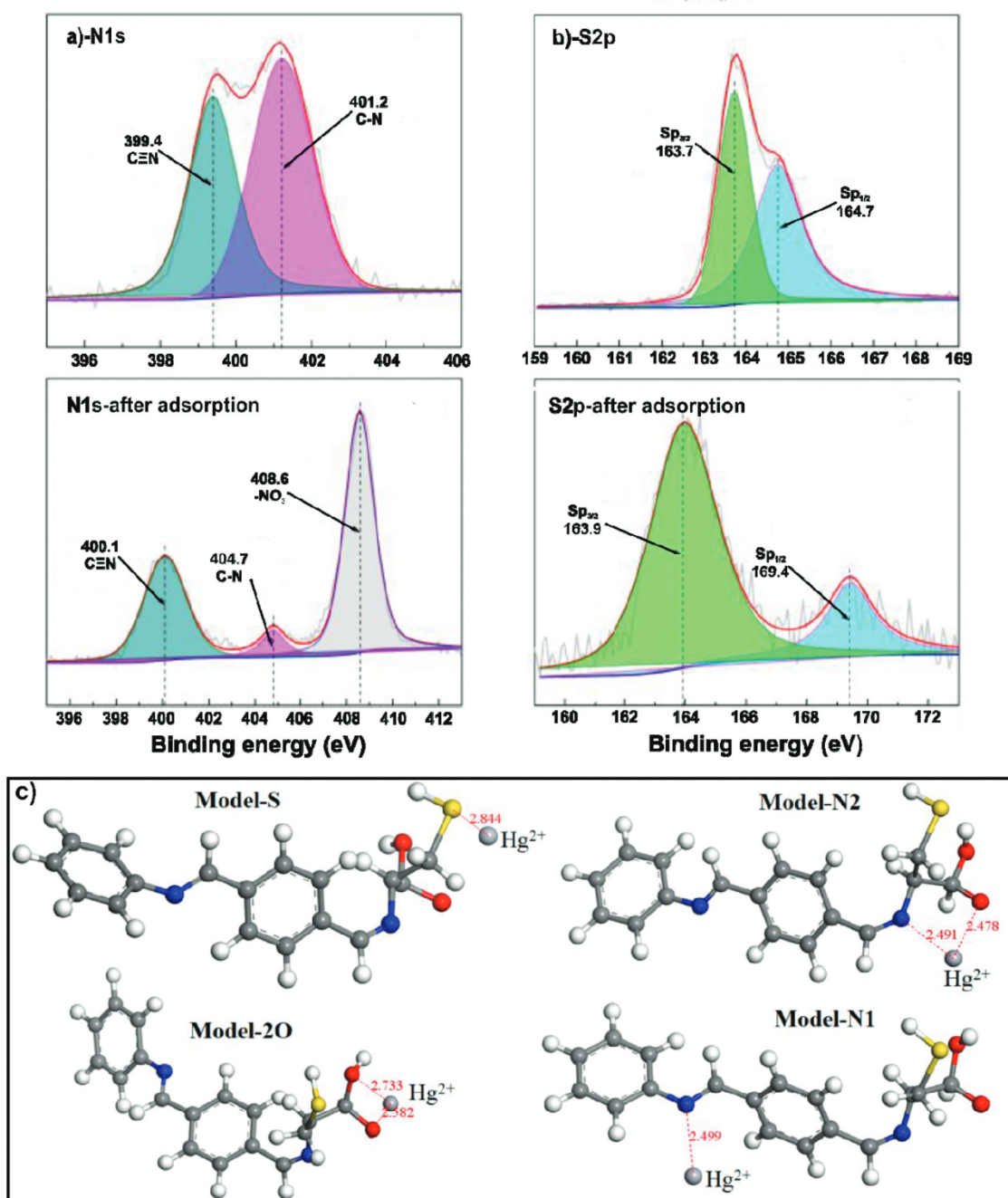


**Figure 5.** (a) High-resolution spectra of N 1s; (b) S 2p before and after Hg<sup>II</sup> adsorption employing Cys-UiO-66; (c) the optimized geometries, binding energies, and bond lengths of Cys-UiO-66 adsorbing Hg<sup>II</sup> at different single ligand binding sites. The gray, white, red, blue, and yellow corresponds to C, H, O, N, S atoms, respectively.

with O-sites was dominant over N-sites or S-sites. The adsorption strength of different functional groups of UiO-66-ATA (Zr) followed the order, hydroxyl > amino > sulphydryl.

#### MOFs for mercury removal

Mercury in the form of methylmercury or ethylmercury is among the most toxic pollutants, with detrimental effects on kidneys, gastrointestinal tract, central nervous system, and heart in humans. The well-known case of 1956 methylmercury poisoning was reported in Minamata City, Japan, where thousands died due to the intake of mercury-contaminated fish and shellfish.<sup>[35,63]</sup> Consequently, designing highly efficient adsorbents for Hg<sup>II</sup> removal is required. Nowadays, researchers are

focused on the development of MOFs, which could be used for selective and versatile capture of Hg<sup>II</sup> ions from wastewater. Li et al.<sup>[48]</sup> studied the outstanding performance of a thiol modified MOF (SH-MIL-68(In)) for Hg<sup>II</sup> removal with a 450 mg g<sup>-1</sup> adsorption capacity. The HRXPS S 2p spectrum of Hg-loaded MOFs showed a shift of 1.2 eV due to a strong coordination between the MOF thiol groups and Hg<sup>II</sup> ions. In another research work, the role of electron-donating N, O, and S atoms in the removal efficiency of Hg<sup>II</sup> was investigated, employing Cys-UiO-66 as the adsorbent. A good 350 mg g<sup>-1</sup> adsorption capacity was reached at pH 5. Considerable positive shifts in the binding energy of functionalities bearing N, O, and S were recorded in their respective HRXPS spectra. These changes

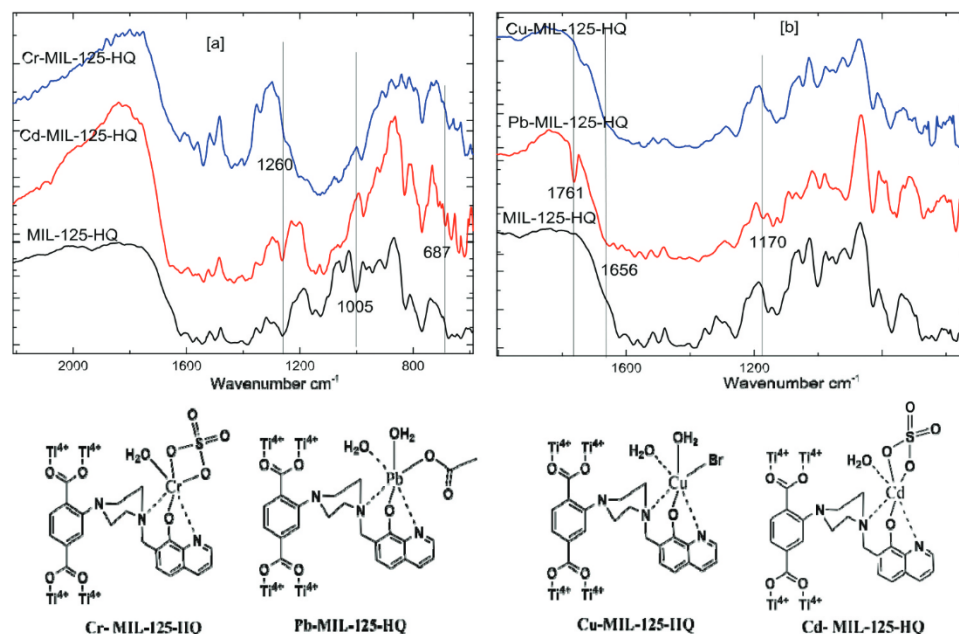


**Figure 6.** The Fourier transform infrared spectra of MIL-125-HQ before and after the adsorption of a) cadmium, and chromium, and b) lead and copper, and bottom, their respective complexes within the MIL-125-HQ framework. With permission from Ref. 87.<sup>[87]</sup> Copyright (2019) Elsevier.

confirmed the involvement of  $-\text{C}=\text{N}$ ,  $-\text{COOH}$ ,  $-\text{OH}$ , and  $-\text{S}-\text{H}$  groups in the  $\text{Hg}^{\text{II}}$  binding process (Figures 5a and b). The DFT energy calculations predicted similar energy for the  $\text{Hg}^{\text{II}}$  binding with different coordination sites (Figure 5c):  $-9.85$  eV (Model-S),  $-8.93$  eV (Model-N1),  $-9.74$  eV (Model-N2), and  $-9.81$  eV (Model-2O). Thus, the DFT study corroborated the XPS analysis, where  $\text{Hg}^{\text{II}}$  ions interacted with the MOF via monodentate (N, S) and bidentate (O) coordination and the S–Hg being the strongest interaction.<sup>[54]</sup>

#### MOFs for chromium removal

The exposure to  $\text{Cr}^{\text{VI}}$  compounds has been associated with mutation and teratogenicity in humans and other living organisms. Chromium is used in leather tanning, alloys manufacturing, cement production, and metal plating. The unregulated effluent discharged from these industrial units into nearby waterbodies is a serious environmental issue.<sup>[66,125]</sup> Therefore, the capture and removal of  $\text{Cr}^{\text{VI}}$  from industrial waste solutions before being discharged is of paramount

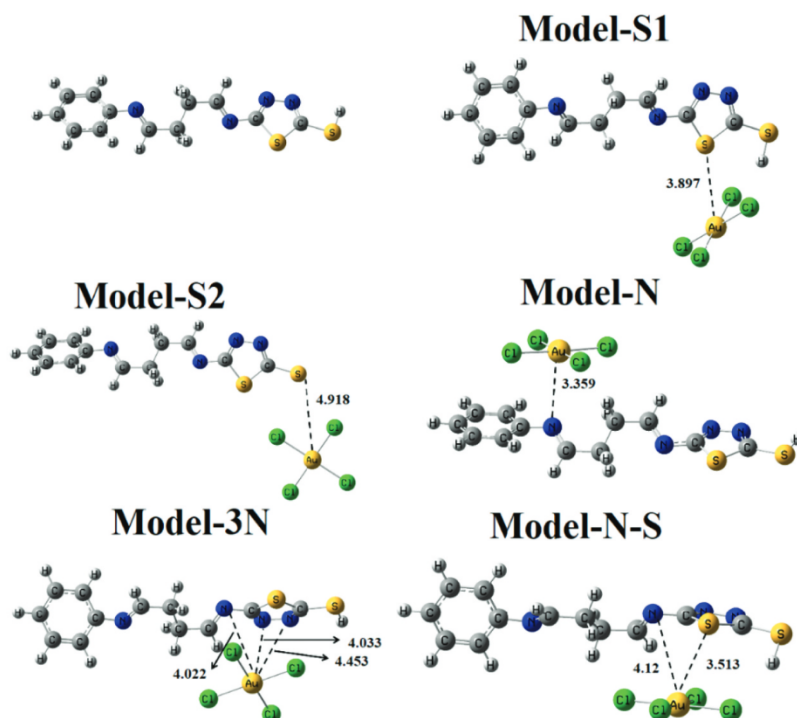


**Figure 7.** The optimized geometries, with distances in Å, of the complexes and the binding energy. Reprinted with permission from Ref. 50.<sup>[50]</sup> Copyright (2020) America Chemical Society.

importance. Some research reports in the literature are focused on finding MOFs for the removal of  $\text{Cr}^{\text{VI}}$  ions. The chromate ( $\text{CrO}_4^{2-}$ ) or dichromate ( $\text{Cr}_2\text{O}_7^{2-}$ ) anions are the negatively charged  $\text{Cr}^{\text{VI}}$  species, which could be captured by the reduction-adsorption process (reduction of  $\text{Cr}^{\text{VI}}$  to  $\text{Cr}^{\text{III}}$ ). Yang et al.<sup>[49]</sup> studied the efficiency of  $\text{Cr}^{\text{VI}}$  adsorption with modified MOFs (Zr-MSA and Zr-DMSA), where the adsorption capacity was 202 and 138  $\text{mg g}^{-1}$  for Zr-MSA and Zr-DMSA, respectively. The HRXPS Cr 2p spectra of Zr-MSA-Cr and Zr-DMSA-Cr showed peaks at 587.0 and 577.3 eV for  $\text{Cr}^{\text{III}}$  ions, indicating that the thiol functionality can reduce  $\text{Cr}^{\text{VI}}$  to  $\text{Cr}^{\text{III}}$  and immobilize it as a  $\text{Cr}^{\text{III}}$ -thiolate complex. The above mechanism was further supported by the presence of peaks for sulfonate groups in the HRXPS S 2p spectrum, arising from the oxidation of thiol groups.

The possible capturing of  $\text{Cr}^{\text{VI}}$  employing  $\text{Fe}_3\text{O}_4@\text{UiO}-66@\text{UiO}67/\text{CTAB}$  as promising adsorbent was reported by Li et al.<sup>[79]</sup> The adsorbent worked well in the wide pH range 1.0–11.0 with the maximum adsorption capacity of 932  $\text{mg g}^{-1}$  at pH 2.0. The HRXPS Cr 2p analysis showed the presence of  $\text{Cr}^{\text{VI}}$  (579.3 and 588.9 eV) and  $\text{Cr}^{\text{III}}$  (577.2 and 586.8 eV) species onto the Cr-loaded MOF composite, suggesting the reduction of a fraction of adsorbed  $\text{Cr}^{\text{VI}}$  ions. Moreover, the C 1s binding energy of  $\text{Fe}_3\text{O}_4@\text{UiO}-66@\text{UiO}67/\text{CTAB}-\text{Cr}$  increased by 1.7 eV, suggesting a decrease in the density of C-electron clouds due to the strong involvement of CTAB in the reduction of  $\text{Cr}^{\text{VI}}$  ions.

#### MOFs for other toxic metals

Other than Pb, Hg, and Cr, many other toxic metals like Cd, As, and Sb are known to have detrimental effects on human health. Binaeian et al.<sup>[44]</sup> developed a novel ZIF-8-mmene for the capture of  $\text{Cd}^{\text{II}}$  ions from wastewater. Its monolayer adsorption capacity of 1000  $\text{mg g}^{-1}$  was found significantly higher than those reported for other MOFs. He et al.<sup>[80]</sup> reported  $\text{UiO}-66(\text{NH}_2)$  for the removal of  $\text{As}^{\text{III}}$  ( $q_m \sim 200 \text{ mg g}^{-1}$ ) and  $\text{As}^{\text{V}}$  ( $q_m \sim 71 \text{ mg g}^{-1}$ ) from wastewater. In the HRXPS Zr 3d spectra, a shift in the binding energy of Zr–O to a lower value suggested the transfer of electron density to the  $\text{As}^{\text{III}}$  and  $\text{As}^{\text{V}}$  species. No shift in the HRXPS N 1s spectra confirmed that the amine functionality was involved in the adsorptive removal of As ions. More information on  $\text{As}^{\text{III}}$  and  $\text{As}^{\text{V}}$  complexes formed with the Zr–O bonds was gathered by EXAFS analysis of  $\text{As}^{\text{III}}-\text{UiO}-66$  and  $\text{As}^{\text{V}}-\text{UiO}-66$ . The As–O shell was formed by 2.4 and 4 oxygen atoms at 1.8 and 1.7 Å in  $\text{As}^{\text{III}}$  and  $\text{As}^{\text{V}}$ , respectively. The As atom in  $\text{As}^{\text{III}}-\text{UiO}-66$  and  $\text{As}^{\text{V}}-\text{UiO}-66$  was surrounded by 1.61 Zr atoms at 3.22 Å and 0.91 Zr atom at 2.95 Å, respectively. Thus, it was concluded that, in this MOF,  $\text{As}^{\text{III}}$  formed bidentate binuclear complexes and  $\text{As}^{\text{V}}$  formed bidentate mononuclear complexes. The MOF adsorbent in a fixed-bed column purified 24 and 19 L of 100 ppb  $\text{As}^{\text{III}}$  and  $\text{As}^{\text{V}}$  solution, respectively, showing its capability to treat As-contaminated groundwater in countries like Bangladesh or India.

Qi et al.<sup>[82]</sup> reported trivalent Sb and As adsorption onto  $\text{Fe}_3\text{O}_4@\text{TA}@\text{UiO}-66$  microspheres as 50  $\text{mg g}^{-1}$  and 98  $\text{mg g}^{-1}$ , respectively. The HRXPS Sb 3d spectrum of  $\text{Fe}_3\text{O}_4@\text{TA}@\text{UiO}-66-\text{Sb}$  confirmed traces of  $\text{Sb}^{\text{V}}$  species apart from a large fraction of  $\text{Sb}^{\text{III}}$  ions onto the adsorbent surface. The HRXPS O 1s

spectra confirmed the involvement of hydroxyl groups of the tannic acid, MOF, and  $\text{Fe}_3\text{O}_4$  in the adsorption of hydroxylated  $\text{Sb}^{\text{III}}$  and  $\text{As}^{\text{III}}$  species via hydrogen bonding. He et al.<sup>[81]</sup> reported significantly high adsorption capacity of  $\text{UiO}-66(\text{NH}_2)$  MOF for  $\text{Sb}^{\text{III}}$  and  $\text{Sb}^{\text{V}}$  within 20 min of equilibration time. In the presence of competing anions such as  $\text{Cl}^-$ ,  $\text{Br}^-$ ,  $\text{NO}_3^-$ ,  $\text{CO}_3^{2-}$ ,  $\text{SO}_4^{2-}$ ,  $\text{H}_2\text{PO}_4^-$ , and  $\text{HPO}_4^{2-}$ , the adsorption capacity of the MOF was not significantly affected for the adsorption of  $\text{As}^{\text{III}}$  ions. But for  $\text{As}^{\text{V}}$  anions,  $\text{SO}_4^{2-}$  and  $\text{HPO}_4^{2-}$  showed a competitive behavior probably due to structural similarities. The MOF showed quantitative removal of antimony from metallurgical wastewater spiked with 10  $\text{mg L}^{-1}$  of Sb ions at pH 7, which confirmed its applicability in the treatment of industrial wastewater.

#### MOFs for multi-metals study

Some researchers focused on the application of functionalized MOFs for the simultaneous adsorptive removal of multiple metals. A MOF with hydroxyquinoline functionalities (MIL-125-HQ) was reported for the adsorptive removal of  $\text{Pb}^{\text{II}}$ ,  $\text{Cd}^{\text{II}}$ ,  $\text{Cu}^{\text{II}}$ , and  $\text{Cr}^{\text{III}}$  with the maximum adsorption capacity of 262, 103, 67, and 54  $\text{mg g}^{-1}$ , respectively. The possible complexation of metal ions by the hydroxyquinoline functionality was reflected in the FTIR spectra Figure 6, where a new band at 830  $\text{cm}^{-1}$  was recorded after the adsorption process.<sup>[87]</sup> Wu et al.<sup>[52]</sup> studied the coordination of  $\text{Eu}^{\text{III}}$ ,  $\text{Hg}^{\text{II}}$ , and  $\text{Pb}^{\text{II}}$  by EDTA ligands anchored onto the  $\text{UiO}-66$  MOF. The  $\text{UiO}-66\text{-EDTA}$  MOF showed an enhanced adsorption capacity of 372 and 358  $\text{mg g}^{-1}$  for  $\text{Hg}^{\text{II}}$  and  $\text{Pb}^{\text{II}}$ , respectively. The binding energy shift of 0.8 and 0.6 eV in the HRXPS O 1s spectrum of  $\text{UiO}-66\text{-EDTA}-\text{Hg}$  and  $\text{UiO}-66\text{-EDTA}-\text{Pb}$ , respectively, confirmed a strong chelation of metal ions with the EDTA O-atoms. From the HRXPS C 1s analysis, it was evident that  $-\text{COOH}$  and C – N from C – N(C)–C played an important role in the coordination of metal ions. The MOF adsorbent nonselectively adsorbed >99% of mixed  $\text{Fe}^{\text{III}}$ ,  $\text{Mn}^{\text{II}}$ ,  $\text{Hg}^{\text{II}}$ ,  $\text{Cd}^{\text{II}}$ ,  $\text{Pb}^{\text{II}}$ ,  $\text{Cu}^{\text{II}}$ ,  $\text{Co}^{\text{II}}$ ,  $\text{Zn}^{\text{II}}$ , and  $\text{Ni}^{\text{II}}$  due to the strong chelation of the EDTA ligand.

#### MOFs for precious metals

Some published works focused on the application of functionalized MOFs for the adsorptive recovery of precious metals like Ag, Au, Pd, and Pt. For the selective recovery of  $\text{Au}^{\text{III}}$  ions, Huang et al.<sup>[83]</sup> developed a ZT-MOF with trithiocyanuric functionalities, where the maximum adsorption capacity reached to 333  $\text{mg g}^{-1}$  at pH 7. The XPS analysis confirmed peaks at 84.36 eV ( $\text{Au } 4f_{7/2}$ ) and 87.36 ( $\text{Au } 4f_{5/2}$ ) for  $\text{Au}^{\text{III}}$  species. The shift in the S binding energy confirmed the interaction of the sulfur-containing functionality with  $\text{Au}^{\text{III}}$  ions. Wan et al.<sup>[50]</sup> designed a novel  $\text{UiO}-66\text{-MTD}$  adsorbent with mercapto-1,3,4-thiodiazole functionality for the recovery of  $\text{Au}^{\text{III}}$  from wastewater. The maximum adsorption capacity reached to 302  $\text{mg g}^{-1}$  at pH 6. The possible regeneration of  $\text{UiO}-66\text{-MTD}-\text{Au}$  and the recovery of adsorbed Au was done by thiourea and HCl. In the HRXPS S 2p spectrum of  $\text{UiO}-66\text{-MTD}-\text{Au}$ , the shifts in S  $2p_{3/2}$  (164.3 eV) and S  $2p_{1/2}$  (168.76 eV) peaks to 163.7 eV and 168.74 eV, respectively, confirmed the major involvement of S-containing functionalities in the  $\text{Au}^{\text{III}}$  chelation. DFT calculations for possible

interaction between UiO-66-MTD and  $\text{AuCl}_4^-$  were carried out with different geometries of the complex Figure 7. Based on energy considerations, it was confirmed that the  $\text{AuCl}_4^-$  ions interacted strongly with the S-containing functionalities through chelate coordination.

In another approach, Zhou et al.<sup>[59]</sup> studied  $\text{NH}_2$ -ZIF-8 for  $\text{Au}^{\text{III}}$  and  $\text{Ag}^{\text{I}}$  recovery. The maximum adsorption capacity of  $\text{NH}_2$ -ZIF-8 for  $\text{Au}^{\text{III}}$  and  $\text{Ag}^{\text{I}}$  was 357 and 222  $\text{mg g}^{-1}$ , respectively. The electrostatic interaction and reduction of noble metal ions onto  $\text{NH}_2$ -ZIF-8 were probed by XPS analysis. In the HRXPS Au 4f spectrum, peaks for  $\text{Au}^{\text{I}}$  (88.7 and 84.25 eV) and  $\text{Au}^{\text{III}}$  (87.19 and 90.61 eV) confirmed a partial reduction of  $\text{Au}^{\text{III}}$  ions. In the HRXPS Ag 3d spectrum, the peaks at 374.1 and 368.1 eV implied a complete reduction of  $\text{Ag}^{\text{I}}$  to  $\text{Ag}^0$ . Both contributions in N 1s signals (C = N and N – H), experienced a shift to lower binding energy after the metal adsorption. Furthermore, the abundance of C = N, N – H, and Zn–OH groups onto  $\text{NH}_2$ -ZIF-8 were responsible for the adsorption and reduction of noble metal ions. For the recovery of  $\text{Pt}^{\text{IV}}$  and  $\text{Pd}^{\text{II}}$  as anions from acidic solutions, MIL-101(Cr)- $\text{NH}_2$  was found effective with significantly higher adsorption capacity (277 and 141  $\text{mg g}^{-1}$  for Pd and Pt, respectively) than its nitro precursor. The MOF adsorbent was successfully used for the recovery of Pd from printed circuit boards and spent catalyst. In the highly acidic leachates of printed boards and spent catalyst, MIL-101(Cr)- $\text{NH}_2$  was able to adsorb 105 and 87  $\text{mg g}^{-1}$  of Pd, respectively, which made the adsorbent highly suitable for the real-world application in recovering noble metals from electronic wastes.<sup>[36]</sup>

### MOFs for rare earth elements

The 14 lanthanides along with yttrium and lanthanum are classified as rare earth elements (REEs). These REEs are extensively used in electronic devices, magnets, batteries, and luminescence devices.<sup>[126]</sup> With the increasing demand, alternative methods are being developed for the pre-concentration of REEs from low-concentrated ores. Also, researchers are keen to recover REEs from discarded electronic equipments, magnets, and batteries. In the literature, fewer reports are available on the application of functionalized MOFs for the adsorptive recovery of trivalent REEs from waste solutions. Lee et al.<sup>[85]</sup> reported  $\text{REE}^{\text{III}}$  adsorption onto different MIL-101 MOF functionalized with an amine, ED, DETA, and PMIDA groups. The  $\text{Gd}^{\text{III}}$  adsorption capacity followed the sequence MIL-101- $\text{NH}_2$  < MIL-101-ED < MIL-101-DETA < MIL-101-PMIDA, which was due to the increasing number of electron-donating atoms. The highest adsorption capacity for MIL-101-PMIDA was due to the presence of synergistic carboxylate ( $-\text{COO}^-$ ) and phosphonic ( $-\text{PO}_3^{2-}$ ) groups, which strongly coordinated with the  $\text{REE}^{\text{III}}$  ions. The trend,  $\text{La}^{\text{III}} < \text{Ce}^{\text{III}} < \text{Nd}^{\text{III}} < \text{Sm}^{\text{III}} < \text{Gd}^{\text{III}}$  was observed for the REEs adsorption capacity onto MIL-101-PMIDA. The DFT calculated bond distance for  $\text{Ln}^{\text{III}}-\text{O}$  is 2.618 and 2.381 Å in  $[\text{La}(\text{H}_2\text{O})_9]^{3+}$  and  $[\text{Lu}(\text{H}_2\text{O})_8]^{3+}$ , respectively.<sup>[127]</sup> Thus, the complexation of  $\text{Gd}^{\text{III}}$  ion with O-atoms of PMIDA [ $\text{Gd}^{\text{III}}\text{-PMIDA}$ ] is expected to be more stable than the complex of  $\text{Sm}^{\text{III}}$  ion [ $\text{Sm}^{\text{III}}\text{-PMIDA}$ ], and the lowest stability is expected for  $[\text{La}^{\text{III}}\text{-PMIDA}]$ . The MIL-101-PMIDA showed a 90% recovery of  $\text{REE}^{\text{III}}$  in the presence of divalent and trivalent transition metal ions.<sup>[85]</sup>

Elsaidi et al.<sup>[84]</sup> synthesized two magnetic MOF microspheres, i.e., magnetite@MIL-101- $\text{SO}_3$  and magnetite@DETA-In-MOF for extracting REEs from aqueous and brine solutions. The extraction ability of magnetite@MIL-101- $\text{SO}_3$  in brine decreased by more than 50% as compared to freshwater. This decrease could be due to the lower selectivity of  $\text{SO}_3^-$  and weaker interaction with  $\text{REE}^{\text{III}}$  in the presence of other competing metal ions and high ionic strength in the brine solution. The magnetite@DETA-In-MOF showed exceptional REE extraction behavior in both water and brine solutions. The DETA ligand is a hard base, which strongly interacts with hard acids like  $\text{REE}^{\text{III}}$ . Thus, DETA ligand, preferentially coordinated with the  $\text{REE}^{\text{III}}$  in the presence of other metal ions in the brine. Thus, it is expected that these functionalized MOFs could be used for the extraction of REEs from waste solutions.

### MOFs for actinides

The three-stage nuclear power program of India is (i) first stage: use of uranium in a pressurized heavy water reactor, (ii) second stage: use of the plutonium generated in the first stage, and (iii) third stage: use of thorium as  $\text{U}^{233}$  generated from the fast breeder reactor. Thus, the recovery of radionuclides of interest (U, Th, and Pu) from nuclear waste solutions, seawater, and minerals are a priority. Seawater accounts for ~99% of the uranium reserves with an average concentration of 3.0  $\mu\text{g L}^{-1}$ . The present technologies are ineffective in extracting U from such a low concentration source due to a low enrichment performance, slow adsorption kinetics, and poor selectivity. The application of MOFs for actinide adsorption is one of the hot topics exclusively focused on the effective recovery of uranium ( $\text{U}^{235}$ ) and thorium ( $\text{Th}^{232}$ ) from nuclear waste solutions or seawater. Though studies dealing with the recovery of Th and U using MOFs are limited, an insight into MOFs possible usage in the recovery of actinides from seawater or other poorly enriched sources was made and deserves a brief discussion.

In the literature, auramine-O (AO) functionalized MOFs have been extensively studied for the preferential adsorption of  $\text{U}^{\text{VI}}$  ions from seawater. Liu et al.<sup>[90]</sup> reported 2.4 times hike in the  $\text{U}^{\text{VI}}$  adsorption capacity of MIL-53(Al) after incorporation of AO groups into MIL-53(Al)- $\text{NH}_2$ , which could be linked to a stronger complex formation of hydroxyl of AO groups with uranyl ions than the N-donating ligands like  $-\text{NH}_2$ . Moreover, MIL-53(Al)-AO showed an increased adsorption performance in the presence of carbonate salts. Since uranium mainly exists as uranyl tricarboxylate complex anion  $[\text{UO}_2(\text{CO}_3)_3]^{4-}$ , the AO functionality could be useful for its recovery from seawater. Wu et al.<sup>[69]</sup> reported  $\text{U}^{\text{VI}}$  adsorption over AO-functionalized MIL-101. The striking feature observed in this study was the remarkable selectivity of MIL-101-OA for the uptake of uranyl ions in the presence of ions generally found in abundance in the seawater (Na, Mg, K, Ca, etc.). Moreover, 0.1 g of MIL-101-OA was able to extract 0.46 mg of uranium from 100 L of natural seawater after 5 days of agitation. Chen et al.<sup>[128]</sup> prepared AO appended UiO-66 (UiO-66-AO) for rapid extraction of uranium from seawater. The UiO-66-AO showed extremely fast uptake of uranyl ions (~99% uptake within 10 min) from the Bohai seawater spiked with 500 ppb U. A mass of 1 mg of

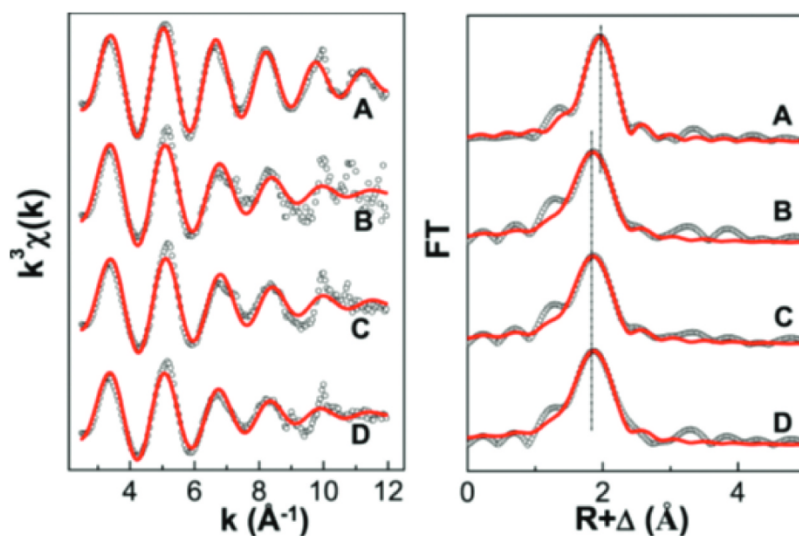


**Figure 8.** Left: raw Th LIII-edge  $k^3$  weighted EXAFS spectra of as-prepared  $\text{Th}^{\text{IV}}$  aqueous solution (A) and  $\text{Th}^{\text{IV}}$ -loaded UiO-66 (B), UiO-66-COOH (C), and UiO-66- $(\text{COOH})_2$  (D). The best theoretical fits are also shown by the red dashed line. Right: corresponding Fourier transforms. Reprinted with permission from Ref. 46.<sup>[46]</sup> Copyright (2020) American Chemical Society.

UiO-66-AO was able to extract  $2.68 \mu\text{g}$  of uranium from 1 L of spiked Bohai seawater after 3 days of stirring.

The carboxylate groups are known to form stronger complexes with  $\text{U}^{\text{VI}}$  ions than the other O-bearing functionalities. Since the MOFs synthetic chemistry is centered on the use of dicarboxylic and tricarboxylic acids/salts as linkers, MOFs synthesized with such linkers should adsorb uranyl ions without functionalization. Feng et al.<sup>[91]</sup> reported the maximum uranyl adsorption capacity of  $332 \text{ mg g}^{-1}$  onto HKUST-1 at pH 6. HKUST-1 ( $\text{Cu}_3(\text{BTC})_2(\text{H}_2\text{O})_3$ ) with BTC as a tricarboxylate ligand has a great number of carboxylate groups, which served as the binding sites for  $\text{U}^{\text{VI}}$  complexation. Li et al.<sup>[74]</sup> adopted a post-synthetic strategy for the transformation of MIL-101-

$\text{NH}_2$  (MOF-1) to carboxyl-functionalized MIL-101 (MOF-3) via a “click reaction.” Though the  $\text{U}^{\text{VI}}$  maximum adsorption capacity of MOF-3 was  $314 \text{ mg g}^{-1}$ , the MOF showed an excellent selectivity in the presence of divalent transition metal ions and trivalent lanthanide ions at pH 7. Wang et al.<sup>[96]</sup> reported ultrafast extraction of uranium from seawater using MOF decorated with acylamide and carboxyl functionalities. 10 mg of their MOF extracted 5.3, 5.1, and  $4.7 \mu\text{g}$  of uranyl ions within 1 min from seawater (pH 7.8, 6 ppb of uranyl concentration) in the three consecutive cycles after regeneration using  $0.1 \text{ mol L}^{-1} \text{ Na}_2\text{CO}_3$ .

Bai et al.<sup>[95]</sup> studied uranyl adsorption onto MIL-101 functionalized with an amine, ED, and DETA as the N-donating

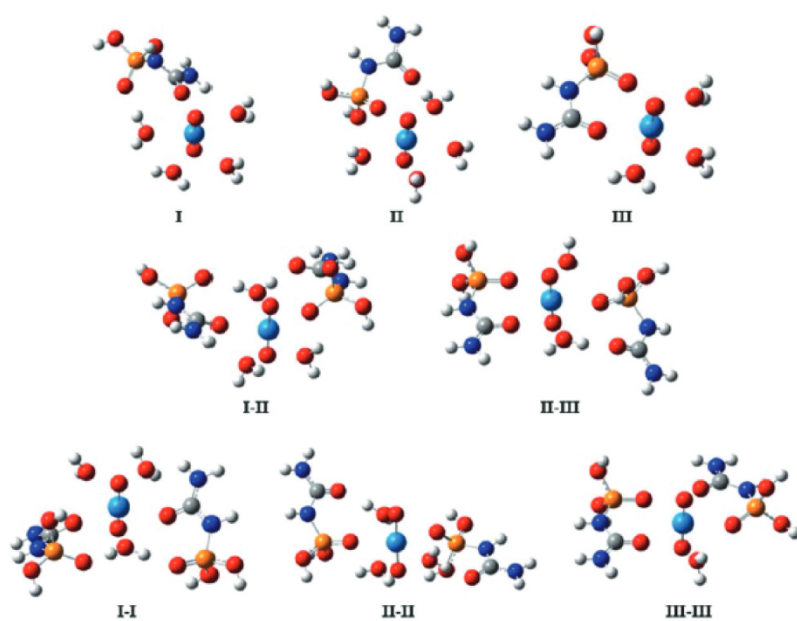


**Figure 9.** Representative structures with optimized binding geometries for the coordination of  $\text{UO}_2^{2+}$  to one and two ligands. In all instances,  $\text{UO}_2^{2+}$  maintains five coordination sites around the equatorial plane. Complexes formed with deprotonated ligands adopted identical structures. Uranium, carbon, nitrogen, oxygen, phosphorus, and hydrogen are light blue, gray, dark blue, red, orange, and white, respectively. Reprinted with permission from Ref. 97.<sup>[97]</sup> Copyright (2020) American Chemical Society.

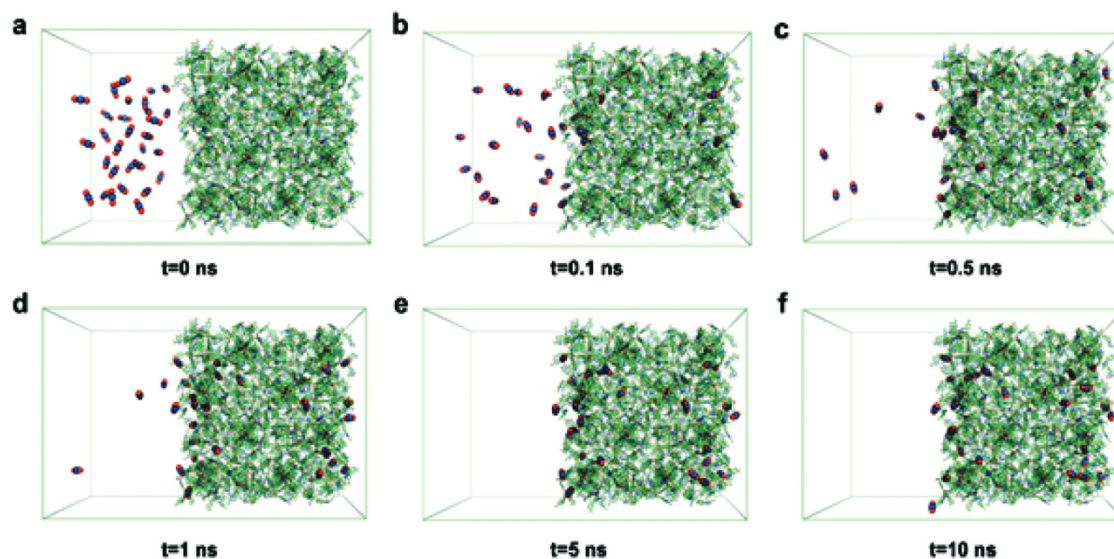


**Figure 10.** Representative snapshots of the  $\text{UO}_2^{2+}$  binding process on MOF-3 during the simulation: (a)  $t = 0$  ns; (b)  $t = 0.1$  ns; (c)  $t = 0.5$  ns; (d)  $t = 1$  ns; (e)  $t = 5$  ns; (f)  $t = 10$  ns. The atoms of uranium and oxygen in uranyl ions are colored in blue and red, respectively. For clear demonstration, the uranyl ions are illustrated as spheres defined by their van der Waals radii, and all water molecules and chloride anions are not shown. Reprinted with permission from Ref. 74.<sup>[74]</sup> Copyright (2020) American Chemical Society..

groups. The adsorption capacity followed the trend: MIL-101-DETA ( $350 \text{ mg g}^{-1}$ ) > MIL-101-ED ( $200 \text{ mg g}^{-1}$ ) > MIL-101-NH<sub>2</sub> ( $90 \text{ mg g}^{-1}$ ), which was completely the reverse of the functional group coverage for these grafted MOFs. The anchoring of amino groups directly to the aromatic rings led to increased steric hindrance and decreased functional activity. Aliphatic amines are more active than aromatic amines. These factors led to a low adsorption capacity of MIL-101-NH<sub>2</sub> for uranyl ions. For MIL-101-ED and MIL-101-DETA, one and two free amino groups were available for the complexation of uranyl ions. MIL-101-DETA with  $0.72 \text{ mol g}^{-1}$  of DETA functional group ( $1.42 \text{ mol g}^{-1}$  of free amino groups) had more accessible binding sites than MIL-101-ED ( $1.28 \text{ mol g}^{-1}$  free amino group), which led to a sufficiently higher adsorption capacity for MIL-101-DETA. Yang et al.<sup>[88]</sup> reported the maximum adsorption capacity of  $200 \text{ mg g}^{-1}$  for azo-MOF, where uranyl ions were complexed with azo and amide functionalities. Tao et al.<sup>[89]</sup> reported ECUT-100 MOF, where the uranyl adsorption was mediated by the amide and azo functionalities.

Li et al.<sup>[92]</sup> followed a direct extraction approach for the recovery of uranium from seawater via anion-exchange mechanism using Co-SLUG-35 as the adsorbent. The ethane disulfonate ( $\text{EDS}^{2-}$ ) anions in Co-SLUG-35 were fully exchanged with  $[\text{UO}_2(\text{CO}_3)_3]^{4-}$  anions at pH 9. In the FTIR spectrum of U-loaded Co-SLUG-35, the disappearance of characteristic absorption bands for  $\text{EDS}^{2-}$ :  $1006, 1040, 1193 \text{ cm}^{-1}$  and the appearance of bands at  $687, 903, 1066, \text{ and } 1415 \text{ cm}^{-1}$  corresponding to  $[\text{UO}_2(\text{CO}_3)_3]^{4-}$ , confirmed the anion-exchange process. The MOF was found selective for anions like  $\text{SO}_4^{2-}$ ,  $\text{NO}_3^-$ , and  $\text{Cl}^-$  but the adsorption capacity decreased from  $89 \text{ mg g}^{-1}$  (in the absence of  $\text{CrO}_4^{2-}$ ) to  $72 \text{ mg g}^{-1}$  (in the presence of  $\text{CrO}_4^{2-}$ ). The MOF showed an extraction efficiency of  $1.0 \text{ mg g}^{-1}$  from 1 L of seawater at pH 8.3, 5.3 ppb U concentration. The best adsorption performance of  $601 \text{ mg g}^{-1}$  was recorded for diaminomaleonitrile (DAMN) functionalized MIL-101 (DSHM-DAMN) at pH 8. The MOF showed

excellent selectivity for uranyl extraction in the presence of alkaline and alkali metal ions found in seawater. The selective extraction of uranium from seawater spiked with  $100 \mu\text{g L}^{-1}$   $\text{U}^{\text{VI}}$  was possible by  $\text{U}^{\text{VI}}$  chelation,  $\text{U}^{\text{VI}}$  being a weaker acid compared to ions like  $\text{Ba}^{2+}$ , or  $\text{Sr}^{2+}$ , by DAMN N-binding sites, weaker bases compared to O-donating ligands like carboxylate or hydroxyl. The HRXPS N 1s spectrum of DSHM-DAMN showed two N-containing functionalities, i.e., C–NH<sub>2</sub> ( $399.6 \text{ eV}$ ) and C≡N ( $398.4 \text{ eV}$ ), which shifted to  $400.5$  and  $399.5 \text{ eV}$ , respectively, after U adsorption. These positive shifts of  $0.9$  and  $1.1 \text{ eV}$  confirmed the strong chelation of uranyl ions by both amino and nitrile functionalities.<sup>[93]</sup>

The magnetic MOF ( $\text{Fe}_3\text{O}_4/\text{AMCA-MIL53}(\text{Al})$ ) that has been applied for actinide recovery was studied by Alqadami et al.,<sup>[98]</sup> where the citric acid was grafted on MIL53(Al) by amidation reaction. The magnetism was possible due to the interaction of one of the carboxylate groups of citric acid with  $\text{Fe}_3\text{O}_4$  nanoparticles. The MOF adsorbent was effectively used for the recovery of  $\text{U}^{\text{VI}}$  ( $227 \text{ mg g}^{-1}$ ) and  $\text{Th}^{\text{IV}}$  ( $286 \text{ mg g}^{-1}$ ) ions. Since  $\text{Th}^{\text{IV}}$  ions are harder acids as compared to  $\text{U}^{\text{VI}}$  ions, the complexation of  $\text{Th}^{\text{IV}}$  was stronger with hard bases like carboxylate and hydroxyl functionalities. Guo et al.<sup>[129]</sup> reported the selective extraction of  $\text{Th}^{\text{IV}}$  from binary solutions of  $\text{Th}^{\text{IV}}$  and  $\text{Ln}^{\text{III}}$  using an uncoordinated salen-containing MOF (dMn-MOFs). Though the MOF showed a low adsorption capacity of  $46 \text{ mg g}^{-1}$ , the separation factor for  $\text{Th}^{\text{IV}}/\text{Eu}^{\text{III}}$  was 16.4 suggesting a possible application for the recovery of Th from lanthanide-rich minerals and nuclear waste solutions. The 1:1 complexation between a  $\text{Th}^{\text{IV}}$  ion and salen, i.e.,  $[\text{Th}(\text{salen})]^{2+}$  was confirmed by the  $m/z \sim 409.2$  peak in electrospray ionization-mass spectroscopy spectrum. Even better separation factors ( $\text{Th}^{\text{IV}}/\text{Ln}^{\text{III}} \sim 6.2\text{--}21.0$ ) were reported for the uncoordinated terpyridine-containing MOF (Ho-MOF), where the  $\text{Th}^{\text{IV}}$  coordination onto the MOF was possible via N-chelating groups.<sup>[73]</sup>

Zhang et al.<sup>[46]</sup> developed mono-carboxylate- and dicarboxylate-bearing UiO-66 for efficient and rapid recovery of Th<sup>IV</sup> ions from weak acidic solutions. The trend for Th<sup>IV</sup> adsorption was: UiO-66-(COOH)<sub>2</sub> > UiO-66-COOH > UiO-66. It followed the carboxylate density required for Th<sup>IV</sup> ion complexation. The study concluded that Th<sup>IV</sup> hydroxides were coordinated with the carboxylate groups of UiO-66-(COOH)<sub>n</sub> (*n* = 1, 2) in the MOF pores via an inner-sphere complexation mechanism. The presence of Th<sup>IV</sup> ions in UiO-66 was linked to its precipitation and DMF exchange with hydrated Th<sup>IV</sup> species. The EXAFS analysis was conducted for Th-loaded MOFs to validate the adsorption mechanisms (Figure 8). The FT peaks at  $\square 2$  Å in spectra B – D shifted toward a lower *R* direction, suggesting involvement of chemical forces in the Th<sup>IV</sup> uptake process. Similar metric parameters were observed for Th-loaded UiO-66-COOH and UiO-66-(COOH)<sub>2</sub>. They suggested a similar Th<sup>IV</sup> coordination in both MOFs. Moreover, the coordination number (C.N.  $\sim 8.1$ ) and the Th–O bond distance (*R*  $\sim 2.4$  Å) for Th-loaded MOFs were lower than those observed for Th<sup>IV</sup> hydrate (C.N.  $\sim 10.5$ , *R*  $\sim 2.46$  Å). These lower values confirmed that the carboxylate-functionalized MOFs adsorbed Th<sup>IV</sup> ions via a chemical process. For UiO-66, a higher C.N.  $\sim 9.4$  and the presence of a small peak at  $\square 3.9$  Å (attributed to backscattering by Th–Th), revealed that the precipitation may have contributed to Th<sup>IV</sup> uptake onto UiO-66.

In some studies, the uranyl–MOF interactions were explored by DFT calculations. Carboni et al.<sup>[97]</sup> performed DFT calculations to investigate the optimized geometries and relative stabilities of U<sup>VI</sup> complexes with carbamoyl-phosphoramidic acid, representative of the metal-binding ligand in MOF 2 and MOF 3. The inter-sorbent distances of 4.5–4.8 Å between carboxyl and phosphoryl oxygen were obtained from the MOF structural models. These distances associated with the large uranyl coordination sphere led to the possibility of U<sup>VI</sup> cooperative binding. Then, seven binding motifs for uranyl ions are possible as represented in Figure 9. Based on the enthalpy consideration, the most favored binding motif was II–II ( $\Delta H_{aq}$   $-197.9$  kcal mol<sup>-1</sup>), where two fully protonated ligands coordinated with the uranyl ion through the phosphoryl oxygen. Coordination motifs I–II ( $\Delta H_{aq}$   $-197.8$  kcal mol<sup>-1</sup>) and I–I ( $\Delta H_{aq}$   $-197.5$  kcal mol<sup>-1</sup>) were slightly less favorable. This study concluded that the binding of uranyl ion with two ligands in the protonated state was more favorable than one ligand. Li et al.<sup>[74]</sup> exploited DFT for studying the uranyl interaction with the carboxylate- and amine-functionalized MIL-101. The uranyl ion interaction with the carboxyl functionality was enthalpically more favorable in the monodentate fashion ( $\Delta H_{aq}$   $-36.9$  to  $-38.0$  kcal mol<sup>-1</sup>) than the bidentate one ( $\Delta H_{aq}$   $-33.1$  kcal mol<sup>-1</sup>). Moreover, the binding affinity of carboxylate functionality for uranyl ions was much higher than the amino functionality ( $\Delta H_{aq}$   $-18.8$  kcal mol<sup>-1</sup>). For this reason, a higher U<sup>VI</sup> adsorption capacity was recorded for MOF-3 in the study.

Li et al.<sup>[74]</sup> studied the underlying microscopic mechanisms for uranyl ions adsorption onto MOF-3 by molecular dynamics (MD) simulation Figure 10. At *t* = 0 or before simulation, all uranyl ions were located in the solution compartment. When

the simulation started, uranyl ions rapidly adsorbed on the surface of MOF-3 and preferentially stayed in the framework rather than moving back to the solution. Within 5 ns, all uranyl ions were extracted from the solution phase into MOF-3 showing rapid establishment of the equilibrium state. Similar MD simulations for amino-functionalized MOF-1 showed incomplete uranyl adsorption even after 30 ns. These results showed a better U<sup>VI</sup> adsorption performance for MOF-3 than for MOF-1. The same inference was made for the protonated MOF-1 and MOF-3 due to the involvement of repulsive force between U<sup>VI</sup> cations and protonated carboxylate groups onto MOF-3 and uranyl ions.<sup>[74]</sup>

Most published works are limited to the recovery of U and Th from seawater and simulated wastewater. Projected MOF applications for the recovery of transuranic elements like neptunium, plutonium, and americium from the high-level radioactive waste solutions are highly dependent on the radiolytic stability of these MOFs. Studies dealing with the radiolytic stability of MOFs are needed to predict the possible applications of MOFs in nuclear waste management. Nonetheless, the existing research works have opened a new domain and possible applications of MOFs for the recovery of valuable uranium from poorly concentrated sources like seawater.

### Challenges, opportunities, and future directions

MOFs have emerged as an alternative to conventional porous adsorbents owing to their large surface area, porosity, high crystallinity, and ease of functionalization. The anchoring of metal ion-specific functionalities onto the MOF is centered around Pearson HSAB theory. Though the grafting of metal-specific N-donor, O-donor, and S-donor functionalities onto the MOF surface is known to lower surface area and porosity, but the functionalization process decreases MOF hydrophobicity, which in turn increases the liquid–solid contact. These functionalized MOFs have shown extraordinary adsorption performances for metal ions of diverse groups and oxidation states, further supported by an excellent selectivity. The MOF adsorption chemistry is a metal ion–ligand interaction governed by complexation, electrostatic interactions, ion-exchange, chelation, hydrogen bonding, and reductive adsorption. Though MOFs show a significant improvement in selectivity, the adsorption capacity is still much lower than those of conventional carbon-based adsorbents like activated carbon and graphene oxide. Another factor is the cost-to-performance evaluation for wastewater remediation, which depends on the MOF synthesis cost, regeneration process, reusability, disposal, and environmental toxicity. These evaluations are mostly absent in the published works. The cost analysis done for the synthesis of UiO-66-NH<sub>2</sub> by Zhao et al.<sup>[54]</sup> was 1.8 USD per MOF gram, which further increased to 6.5 USD per gram for Cys-UiO-66, showing the significant cost of functionalization. The overall synthesis cost of a MOF is significantly higher than that of any commercial adsorbents and ion-exchangers. So, in the present conditions, it is hard to label a MOF, an economic adsorbent for heavy metal removal. Another concern regarding MOFs is their structural stability in water, which affects the performance and may increase the toxicity as well. This MOF toxicity is another

concern which needs thorough evaluation before MOFs being used in the wastewater treatment.

The literature lacks substantial information on the adsorptive recovery of precious metals and REEs using functionalized MOFs. The only study on the practical application of MOFs for such recovery was reported by Lim et al.<sup>[36]</sup> Their MOF adsorbent was able to extract a significant amount of Pd from the acidic leachates of discarded PCBs and spent catalysts. This demonstrates that acid-resistant MOFs could be considered as economically viable adsorbents for the preconcentration or recovery of noble metals and REEs from discarded consumer products especially electronic devices. The use of MOFs for sequestration of uranium and thorium from seawater is attractive and could become a success story if the same performance and selectivity of MOF are reflected in scale-up studies. These functionalized MOF adsorbents showed extraordinary recovery of radionuclides from poorly concentrated seawater. It is still a challenge to recover these actinides from spent nuclear fuels. So far, the radio-stability of MOFs is undocumented. The radio-stability of MOFs against high-energy particles and gamma radiation needs systematic evaluation for these adsorbents to be used in the recovery process of the nuclear fuel cycle. This could be translated for the recovery of radionuclides like plutonium and americium. In the future, we hope for the development of radiolytically stable MOFs, which could be used for nuclear waste decontamination and actinide recovery from seawater.

The scarce information in the literature for real-world MOF applications in wastewater treatment should not be the criteria for ruling out their use and commercialization in the future. The need is to develop green and stable MOFs through cost-effective approaches, which may overcome many issues. Column and pilot-scale studies for the treatment of industrial wastewater using MOFs coupled with their cost-to-performance evaluation could help researchers to comment on the large-scale applicability of these adsorbents. Studies on the biological toxicity of MOFs will be the deciding factor in their potential utilization in wastewater treatment facilities. The integration of these modified MOFs into columns, membranes, and filter components could pave the way for advanced devices. The original properties of MOF: high porosity, sorption selectivity, stability, and reusability could be combined for their application in wastewater treatment plants. Moreover, MOFs could serve as novel platforms for grafting specific functionalities to recover precious noble metals and rare earth elements from low concentrated ore leachates. This could limit the use of toxic chemicals in the entire process (like the use of toxic cyanide ions in the recovery of gold).

Current technologies in the removal of heavy metals are centered on the use of activated carbon as the solid-phase adsorbent or the use of chemicals as precipitating agents in wastewater treatment facilities. These processes generate high volumes of toxic sludge. The disposal treatment of this sludge increases the operational cost along with possible contamination of the disposal site. MOF-integrated filters could be a possible solution to remove toxic heavy metals without generating sludge. The preconcentration and recovery of precious metals including rare earth elements from ore leachates are some of the hot topics of the decade. This has been triggered by the booming electronic industry coupled with the need to be self-reliant by recycling resources. As such, MOFs developed

from common linkers are not very selective toward a particular metal ion. The ability to incorporate metal-specific functionalities make them an important candidate for the solid-phase extraction of precious metals, which up to now has been more or less dependent on liquid-phase extraction involving the use of toxic chemicals. Today, actinide extraction from seawater is far from reality, mostly due to the ultra-low concentration of U and Th in seawater with a significantly higher concentration of other metal salts. MOFs anchored with specific organic functionalities have shown potential in capturing Th and U and enriching seawater. Although these studies are limited in number, the recent growth in the field could lead to possible commercialization soon. Also, the reprocessing of spent nuclear waste to recover precious radionuclides of Th, U, Pu, and Am is a challenging task. The high-energy radiations deteriorate the structural integrity of the materials that makes the process obsolete. So far, radiochemists are exclusively use liquid-liquid extraction for reprocessing of spent fuel, but the process has been challenged due to its poor reusability. Although the literature lacks systematic studies on the use of MOFs for actinide recovery in real nuclear waste solutions, recent reports on the gamma-stability of MOFs could be the starting point for exploring MOFs for nuclear waste decontamination. Based on the scattered and scarce literature, it is hard to predict possible direction for MOF applications in the nuclear industry, but MOFs certainly have the potential to be used for the preconcentration of rare earth, noble metals, and actinides from their respective trace sources.

## Conclusions

This review summarizes the development of functionalized MOFs for their novel application in the adsorptive removal or recovery of heavy metals, precious metals, rare earth elements, and radioactive actinides from wastewater and poorly concentrated reserves. The literature is enriched with different pre- and post-functionalization strategies for the development of functionalized MOFs meant for removal and recovery of specific metal ions. An overview of the novel and updated methods for preparing functionalized MOFs is provided. The discussion on the synthetic routes was mainly focused on the organic linkers and their role as selective metal-binding sites. The influence of physicochemical properties on the adsorptive performance of the material is briefly discussed where surface area, pore size, and water stability played a crucial role in efficient metal loading. In most cases, the adsorption of metal ions by MOFs was governed by complexation and coordination with some reports on the possibility of electrostatic interactions, which were supported by spectroscopic and computational evidence. The selectivity and reusability of the functionalized MOFs turned out to be a determinant factor on the overall efficiency of the adsorption process. Despite a high cost and some practical difficulties, functionalized MOFs are very promising materials for water treatment, particularly for the enrichment of precious metals and actinides from poorly concentrated sources. There are several MOFs that qualify for their applications in the enrichment process. Detail column studies and their applications in real solutions should be explored for a better judgment of MOFs and their role in the

domain of separation and purification technology.

## Acknowledgments

N.K.G would like to thank the University of Science and Technology and Department of Land, Water, and Environment Research, Korea Institute of Civil Engineering and Building Technology. H.V., Y.C.L., C.L., R. P. would like to thank the Laboratorio Nacional de Conversión y Almacenamiento de Energía (LNCAE) and Laboratorio Nacional de la Ciencia, Tecnología y Gestión del Agua (LNAGUA) from Centro de Investigación en Ciencia Aplicada y Tecnología Avanzada de Mexico.

## Funding

This research did not receive any specific grant from funding agencies in the public, commercial, or not-for-profit sectors.

## ORCID

Carolina Leyva  <http://orcid.org/0000-0003-4327-9569>

## References

- [1] Li, J.; Wang, X.; Zhao, G.; Chen, C.; Chai, Z.; Alsaedi, A.; Hayat, T.; Wang, X. Metal-Organic Framework-Based Materials: Superior Adsorbents for the Capture of Toxic and Radioactive Metal Ions. *Chem. Soc. Rev.* **2018**, *47*, 2322–2356. DOI: [10.1039/C7CS00543A](https://doi.org/10.1039/C7CS00543A).
- [2] Duru, İ.; Ege, D.; Kamali, A. R. Graphene Oxides for Removal of Heavy and Precious Metals from Wastewater. *J. Mater. Sci.* **2016**, *51*(13), 6097–6116. DOI: [10.1007/s10853-016-9913-8](https://doi.org/10.1007/s10853-016-9913-8).
- [3] Tauetsile, P. J.; Oraby, E. A.; Eksteen, J. J. Activated Carbon Adsorption of Gold from Cyanide-Starved Glycine Solutions Containing Copper. Part 1: Isotherms. *Sep. Purif. Technol.* **2019**, *211*, 594–601. DOI: [10.1016/j.seppur.2018.09.024](https://doi.org/10.1016/j.seppur.2018.09.024).
- [4] Sung, J.-H.; Back, S.-K.; Lee, E.-S.; Jang, H.-N.; Seo, Y.-C.; Kang, Y.-S.; Lee, M.-H. Application of Powdered Activated Carbon Coating to Fabrics in a Hybrid Filter to Enhance Mercury Removal. *J. Environ. Sci.* **2019**, *80*, 58–65. DOI: [10.1016/j.jes.2018.08.004](https://doi.org/10.1016/j.jes.2018.08.004).
- [5] Mukkata, K.; Kantachote, D.; Wittayaweerassak, B.; Megharaj, M.; Naidu, R. The Potential of Mercury Resistant Purple Nonsulfur Bacteria as Effective Biosorbents to Remove Mercury from Contaminated Areas. *Biocatal. Agric. Biotechnol.* **2019**, *17*, 93–103. DOI: [10.1016/j.bcab.2018.11.008](https://doi.org/10.1016/j.bcab.2018.11.008).
- [6] De Freitas, G. R.; Vieira, M. G. A.; Da Silva, M. G. C. Fixed Bed Biosorption of Silver and Investigation of Functional Groups on Acidified Biosorbent from Algae Biomass. *Environ. Sci. Pollut. Res.* **2019**, *26*, 36354–36366. DOI: [10.1007/s11356-019-06731-5](https://doi.org/10.1007/s11356-019-06731-5).
- [7] Xu, H.; Yuan, H.; Yu, J.; Lin, S. Study on the Competitive Adsorption and Correlational Mechanism for Heavy Metal Ions Using the Carboxylated Magnetic Iron Oxide Nanoparticles (MNPs-COOH) as Efficient Adsorbents. *Appl. Surf. Sci.* **2019**, *473*, 960–966. DOI: [10.1016/j.apsusc.2018.12.006](https://doi.org/10.1016/j.apsusc.2018.12.006).
- [8] Arshad, F.; Selvaraj, M.; Zain, J.; Banat, F.; Haija, M. A. Polyethylenimine Modified Graphene Oxide Hydrogel Composite as an Efficient Adsorbent for Heavy Metal Ions. *Sep. Purif. Technol.* **2019**, *209*, 870–880. DOI: [10.1016/j.seppur.2018.06.035](https://doi.org/10.1016/j.seppur.2018.06.035).
- [9] Neyestani, M. R.; Shemirani, F.; Mozaffari, S.; Alvand, M. A Magnetized Graphene Oxide Modified with 2-Mercaptobenzothiazole as A Selective Nanosorbent for Magnetic Solid Phase Extraction of Gold(III), Palladium(II) and Silver(I). *Microchim. Acta.* **2017**, *184*, 2871–2879. DOI: [10.1007/s00604-017-2299-8](https://doi.org/10.1007/s00604-017-2299-8).
- [10] Hoskins, B. F.; Robson R. Design and Construction of A New Class of Scaffolding-Like Materials Comprising Infinite Polymeric Frameworks of 3D-Linked Molecular Rods. A Reappraisal of the Zn(CN)<sub>2</sub> and Cd(CN)<sub>2</sub> Structures and the Synthesis and Structure of the Diamond-Related Framework. *J. Am. Chem. Soc.* **1990**, *112* (4), 1546–1554. DOI: [10.1021/ja00160a038](https://doi.org/10.1021/ja00160a038).
- [11] Kinoshita, Y.; Matsubara, I.; Higuchi, T.; Saito, Y. The Crystal Structure of Bis(Adiponitrilo)copper(I) Nitrate. *Bull. Chem. Soc. Jpn.* **1959**, *32*(11), 1221–1226. DOI: [10.1246/bcsj.32.1221](https://doi.org/10.1246/bcsj.32.1221).
- [12] Robson, R.; Design and Its Limitations in the Construction of Bi- and Poly-Nuclear Coordination Complexes and Coordination Polymers (Aka MOFs): A Personal View. *Dalton Trans.* **2008**, *38*, 5113–5131. DOI: [10.1039/B805617J](https://doi.org/10.1039/B805617J).
- [13] Li, H.; Eddaoudi, M.; O’Keeffe, M.; Yaghi, O. M. Design and Synthesis of an Exceptionally Stable and Highly Porous Metal-Organic Framework. *Nature.* **1999**, *402*, 276–279. DOI: [10.1038/46248](https://doi.org/10.1038/46248).
- [14] Chui, S. S.-Y.; Lo, S. M.-F.; Charmant, J. P. H.; Orpen, A. G.; Williams, I. D. A Chemically Functionalizable Nanoporous Material [Cu<sub>3</sub>(tma)<sub>2</sub>(H<sub>2</sub>O)<sub>3</sub>]<sub>n</sub>. *Science.* **1999**, *283*(5405), 1148–1150. DOI: [10.1126/science.283.5405.1148](https://doi.org/10.1126/science.283.5405.1148).
- [15] Barthelet, K.; Marrot, J.; Riou, D.; Férey, G.; Breathing Hybrid, A. Organic-Inorganic Solid with Very Large Pores and High Magnetic Characteristics. *Angew. Chem., Int. Ed.* **2002**, *41*(2), 281–284.
- [16] Serre, C.; Millange, F.; Thouvenot, C.; Noguès, M.; Marsolier, G.; Louër, D.; Férey, G.; Very Large Breathing Effect in the First Nanoporous Chromium(III)-Based Solids, MIL-53 or Cr<sup>III</sup>(OH)-{O<sub>2</sub>C-C<sub>6</sub>H<sub>4</sub>-CO<sub>2</sub>}-{HO<sub>2</sub>C-C<sub>6</sub>H<sub>4</sub>-CO<sub>2</sub>H}<sub>x</sub>-H<sub>2</sub>O<sub>y</sub>. *J. Am. Chem. Soc.* **2002**, *124*45, 13519–13526. DOI: [10.1021/ja0276974](https://doi.org/10.1021/ja0276974).
- [17] Tian, Y.-Q.; Cai, C.-X.; Ji, Y.; You, X.-Z.; Peng, S.-M.; Lee, G.-H. [Co<sub>5</sub>(im)<sub>10</sub>-2mb]<sub>∞</sub>: A Metal-Organic Open-Framework with Zeolite-Like Topology. *Angew. Chem., Int. Ed.* **2002**, *41*(8), 1384–1386.
- [18] Hupp, J. T.; Poeppelmeler, K. R. Better Living Through Nanopore Chemistry. *Science.* **2005**, *309*(5743), 2008–2009. DOI: [10.1126/science.1117808](https://doi.org/10.1126/science.1117808).
- [19] Cavka, J. H.; Jakobsen, S.; Olsbye, U.; Guillou, N.; Lamberti, C.; Bordiga, S.; Lillerud, K. P. A New Zirconium Inorganic Building Brick Forming Metal Organic Frameworks with Exceptional Stability. *J. Am. Chem. Soc.* **2008**, *130*(42), 13850–13851. DOI: [10.1021/ja8057953](https://doi.org/10.1021/ja8057953).
- [20] Bonneau, M.; Lavenn, C.; Ginet, P.; Otake, K.; Kitagawa, S. Upscale Synthesis of a Binary Pillared Layered MOF for Hydrocarbon Gas Storage and Separation. *Green Chem.* **2020**, *22*, 718–724. DOI: [10.1039/C9GC03561C](https://doi.org/10.1039/C9GC03561C).
- [21] Wang, Q.; Liu, Q.; Du, X.-M.; Zhao, B.; Li, Y.; Ruan, W.-J.; White-Light-Emitting Single, A. MOF Sensor-Based Array for Berberine Homologue Discrimination. *J. Mater. Chem. C.* **2020**, *8*, 1433–1439. DOI: [10.1039/C9TC05180E](https://doi.org/10.1039/C9TC05180E).
- [22] Jrad, A.; Hmadeh, M.; Tarboush, B. J. A.; Awada, G.; Ahmad, M. Structural Engineering of Zr-Based Metal-Organic Framework Catalysts for Optimized Biofuel Additives Production. *Chem. Eng. J.* **2020**, *382*, 122793. DOI: [10.1016/j.cej.2019.122793](https://doi.org/10.1016/j.cej.2019.122793).
- [23] Chueh, -C.-C.; Chen, C.-I.; Su, Y.-A.; Konnerth, H.; Gu, Y.-J.; Kung, C.-W.; Wu, K. C.-W. Harnessing MOF Materials in Photovoltaic Devices: Recent Advances, Challenges, and Perspectives. *J. Mater. Chem. A.* **2019**, *7*, 17079–17095. DOI: [10.1039/C9TA03595H](https://doi.org/10.1039/C9TA03595H).
- [24] Lee, -C.-C.; Chen, C.-I.; Liao, Y.-T.; Wu, K. C.-W.; Chueh, -C.-C. Enhancing Efficiency and Stability of Photovoltaic Cells by Using Perovskite/Zr-MOF Heterojunction Including Bilayer and Hybrid Structures. *Adv. Sci.* **2019**, *6*(5), 1801715. DOI: [10.1002/adv.201801715](https://doi.org/10.1002/adv.201801715).
- [25] Orellana-Tavira, C.; Köppen, M.; Li, A.; Stock, N.; Fairen-Jimenez, D. Biocompatible Crystalline, and Amorphous Bismuth-Based Metal-Organic Frameworks for Drug Delivery. *ACS Appl. Mater. Interfaces.* **2020**, *12*(5), 5633–5641. DOI: [10.1021/acsami.9b21692](https://doi.org/10.1021/acsami.9b21692).
- [26] Joseph, L.; Jun, B.-M.; Jang, M.; Park, C. M.; Muñoz-Senmache, J. C.; Hernández-Maldonado, A. J.; Heyden, A.; Yu, M.; Yoon, Y. Removal of Contaminants of Emerging Concern by Metal-Organic Framework Nanoadsorbents: A Review. *Chem. Eng. J.* **2019**, *369*, 928–946. DOI: [10.1016/j.cej.2019.03.173](https://doi.org/10.1016/j.cej.2019.03.173).

- [27] Sini, K.; Bourgeois, D.; Idouhar, M.; Carboni, M.; Meyer, D. Metal-Organic Frameworks Cavity Size Effect on the Extraction of Organic Pollutants. *Mater. Lett.* **2019**, *250*, 92–95. DOI: [10.1016/j.matlet.2019.04.113](https://doi.org/10.1016/j.matlet.2019.04.113).
- [28] Yu, W.; Luo, M.; Yang, Y.; Wu, H.; Huang, W.; Zeng, K.; Luo, F. Metal-Organic Framework (MOF) Showing Both Ultrahigh As(V) and As(III) Removal from Aqueous Solution. *J. Solid State Chem.* **2019**, *269*, 264–270. DOI: [10.1016/j.jssc.2018.09.042](https://doi.org/10.1016/j.jssc.2018.09.042).
- [29] Ma, J.; Li, S.; Wu, G.; Wang, S.; Guo, X.; Wang, L.; Wang, X.; Li, J.; Chen, L. Preparation of Mixed-Matrix Membranes from Metal Organic Framework (MIL-53) and Poly (Vinylidene Fluoride) for Use in Determination of Sulfonyleurea Herbicides in Aqueous Environments by High Performance Liquid Chromatography. *J. Colloid Interface Sci.* **2019**, *553*, 834–844. DOI: [10.1016/j.jcis.2019.06.082](https://doi.org/10.1016/j.jcis.2019.06.082).
- [30] Wu, G.; Ma, J.; Li, S.; Wang, S.; Jiang, B.; Luo, S.; Li, J.; Wang, X.; Guan, Y.; Chen, L. Cationic Metal-Organic Frameworks as an Efficient Adsorbent for the Removal of 2,4-Dichlorophenoxyacetic Acid from Aqueous Solutions. *Environ. Res.* **2020**, *186*, 109542. DOI: [10.1016/j.envres.2020.109542](https://doi.org/10.1016/j.envres.2020.109542).
- [31] Wu, G.; Ma, J.; Wang, S.; Chai, H.; Guo, L.; Li, J.; Ostovan, A.; Guan, Y.; Chen, L. Cationic Metal-Organic Framework Based Mixed-Matrix Membrane for Extraction of Phenoxy Carboxylic Acid (PCA) Herbicides from Water Samples Followed by UHPLC-MS/MS Determination. *J. Hazard. Mater.* **2020**, *394*, 122556. DOI: [10.1016/j.jhazmat.2020.122556](https://doi.org/10.1016/j.jhazmat.2020.122556).
- [32] Navarathna, C. M.; Dewage, N. B.; Karunanayake, A. G.; Farmer, E. L.; Perez, F.; Hassan, E. B.; Mlsna, T. E.; Pittman, J.; Rhodamine B, C. U. Adsorptive Removal and Photocatalytic Degradation on MIL-53-Fe MOF/Magnetic Magnetite/Biochar Composites. *J. Inorg. Organomet. Polym. Mater.* **2020**, *30*, 214–229. DOI: [10.1007/s10904-019-01322-w](https://doi.org/10.1007/s10904-019-01322-w).
- [33] Chen, Y.; Zhai, B. Y.; Liang, Y. N.; Li, Y. Hybrid Photocatalysts Using Semiconductor/MOF/Graphene Oxide for Superior Photodegradation of Organic Pollutants under Visible Light. *Mater. Sci. Semicond. Process.* **2020**, *107*, 104838. DOI: [10.1016/j.mssp.2019.104838](https://doi.org/10.1016/j.mssp.2019.104838).
- [34] Zheng, M.; Zhao, X.; Wang, K.; She, Y.; Gao, Z. Highly Efficient Removal of Cr(VI) on a Stable Metal-Organic Framework Based on Enhanced H-Bond Interaction. *Ind. Eng. Chem. Res.* **2019**, *58* (51), 23330–23337. DOI: [10.1021/acs.iecr.9b04598](https://doi.org/10.1021/acs.iecr.9b04598).
- [35] Hasankola, Z. S.; Rahimi, R.; Shayegan, H.; Moradi, E.; Safarifar, V. Removal of Hg<sup>2+</sup> Heavy Metal Ion Using a Highly Stable Mesoporous Porphyrinic Zirconium Metal-Organic Framework. *Inorganica Chim. Acta.* **2020**, *501*, 119264. DOI: [10.1016/j.ica.2019.119264](https://doi.org/10.1016/j.ica.2019.119264).
- [36] Lim, C.-R.; Lin, S.; Yun, Y.-S. Highly Efficient and Acid-Resistant Metal-Organic Frameworks of MIL-101(Cr)-NH<sub>2</sub> for Pd(II) and Pt(IV) Recovery from Acidic Solutions: Adsorption Experiments, Spectroscopic Analyses, and Theoretical Computations. *J. Hazard. Mater.* **2020**, *387*, 121689. DOI: [10.1016/j.jhazmat.2019.121689](https://doi.org/10.1016/j.jhazmat.2019.121689).
- [37] Shao, Z.; Huang, C.; Wu, Q.; Zhao, Y.; Xu, W.; Liu, Y.; Dang, J.; Hou, H. Ion Exchange Collaborating Coordination Substitution: More Efficient Cr(VI) Removal Performance of a Water-Stable Cu<sup>II</sup>-MOF Material. *J. Hazard. Mater.* **2019**, *378*, 120719. DOI: [10.1016/j.jhazmat.2019.05.112](https://doi.org/10.1016/j.jhazmat.2019.05.112).
- [38] Meng, L.; Yang, L.; Chen, C.; Dong, X.; Ren, S.; Li, G.; Li, Y.; Han, Y.; Shi, Z.; Feng, S. Selective Acetylene Adsorption within an Imino-Functionalized Nanocage-Based Metal-Organic Framework. *ACS Appl. Mater. Interfaces.* **2020**, *12*(5), 5999–6006. DOI: [10.1021/acsami.9b21938](https://doi.org/10.1021/acsami.9b21938).
- [39] Ghosh, A.; Das, G. Green Synthesis of Sn(II)-BDC MOF: Preferential and Efficient Adsorption of Anionic Dyes. *Microporous Mesoporous Mater.* **2020**, *297*, 110039. DOI: [10.1016/j.micromeso.2020.110039](https://doi.org/10.1016/j.micromeso.2020.110039).
- [40] Wan, Y.; Wan, J.; Ma, Y.; Wang, Y.; Luo, T. Sustainable Synthesis of Modulated Fe-MOFs with Enhanced Catalyst Performance for Persulfate to Degrade Organic Pollutants. *Sci. Total Environ.* **2020**, *701*, 134806. DOI: [10.1016/j.scitotenv.2019.134806](https://doi.org/10.1016/j.scitotenv.2019.134806).
- [41] De Lima Neto, O. J.; Frós, A. C.; De, O.; Barros, B. S.; De Farias Monteiro, A. F.; Kulesza, J. Rapid and Efficient Electrochemical Synthesis of a Zinc-Based Nano-MOF for Ibuprofen Adsorption. *New J. Chem.* **2019**, *43*, 5518–5524. DOI: [10.1039/C8NJ06420B](https://doi.org/10.1039/C8NJ06420B).
- [42] Luo, X.; Mai, Z.; Lei, H.; Bifunctional Luminescent, A. Zn(II)-Organic Framework: Ionothermal Synthesis, Selective Fe(III) Detection and Cationic Dye Adsorption. *Inorg. Chem. Commun.* **2019**, *102*, 215–220. DOI: [10.1016/j.inoche.2019.02.033](https://doi.org/10.1016/j.inoche.2019.02.033).
- [43] Chen, Y.; Wu, H.; Yuan, Y.; Lv, D.; Qiao, Z.; An, D.; Wu, X.; Liang, H.; Li, Z.; Xia, Q. Highly Rapid Mechanochemical Synthesis of a Pillar-Layer Metal-Organic Framework for Efficient CH<sub>4</sub>/N<sub>2</sub> Separation. *Chem. Eng. J.* **2020**, *385*, 123836. DOI: [10.1016/j.cej.2019.123836](https://doi.org/10.1016/j.cej.2019.123836).
- [44] Binaeian, E.; Maleki, S.; Motaghedi, N.; Arjmandi, M. Study on the Performance of Cd<sup>2+</sup> Sorption Using Dimethylethylenediamine-Modified Zinc-Based MOF (Zif-8-mm): Optimization of the Process by RSM Technique. *Sep. Sci. Technol.* **2020**, *55*(15), 2713–2728. DOI: [10.1080/01496395.2019.1655056](https://doi.org/10.1080/01496395.2019.1655056).
- [45] Zhang, R.; Liu, Y.; An, Y.; Wang, Z.; Wang, P.; Zheng, Z.; Qin, X.; Zhang, X.; Dai, Y.; Huang, B.; et al. Metal-Organic Framework as an Efficient Adsorbent of Pb(II) Ions. *Colloids Surf., A.* **2019**, *560*, 315–322. DOI: [10.1016/j.colsurfa.2018.10.011](https://doi.org/10.1016/j.colsurfa.2018.10.011).
- [46] Zhang, N.; Yuan, L.-Y.; Guo, W.-L.; Luo, S.-Z.; Chai, Z.-F.; Shi, W.-Q. Extending the Use of Highly Porous and Functionalized MOFs to Th(IV) Capture. *ACS Appl. Mater. Interfaces.* **2017**, *9*(30), 25216–25224. DOI: [10.1021/acsami.7b04192](https://doi.org/10.1021/acsami.7b04192).
- [47] Hua, W.; Zhang, T.; Wang, M.; Zhu, Y.; Wang, X. Hierarchically Structural PAN/UiO-66-(COOH)<sub>2</sub> Nanofibrous Membranes for Effective Recovery of Terbium(III) and Europium(III) Ions and Their Photoluminescence Performances. *Chem. Eng. J.* **2019**, *370*, 729–741. DOI: [10.1016/j.cej.2019.03.255](https://doi.org/10.1016/j.cej.2019.03.255).
- [48] Li, G.-P.; Zhang, K.; Zhang, P.-F.; Liu, W.-N.; Tong, W.-Q.; Hou, L.; Wang, -Y.-Y. Thiol-Functionalized Pores via Post-Synthesis Modification in a Metal-Organic Framework with Selective Removal of Hg(II) in Water. *Inorg. Chem.* **2019**, *58*(5), 3409–3415. DOI: [10.1021/acs.inorgchem.8b03505](https://doi.org/10.1021/acs.inorgchem.8b03505).
- [49] Yang, P.; Shu, Y.; Zhuang, Q.; Li, Y.; Gu, J. Metal-Organic Frameworks Bearing Dense Alkyl Thiol for the Efficient Degradation and Concomitant Removal of Toxic Cr(VI). *Langmuir.* **2019**, *35*(49), 16226–16233. DOI: [10.1021/acs.langmuir.9b03057](https://doi.org/10.1021/acs.langmuir.9b03057).
- [50] Wang, C.; Lin, G.; Zhao, J.; Wang, S.; Zhang, L. Enhancing Au(III) Adsorption Capacity and Selectivity via Engineering MOF with Mercapto-1,3,4-Thiadiazole. *Chem. Eng. J.* **2020**, *388*, 124221. DOI: [10.1016/j.cej.2020.124221](https://doi.org/10.1016/j.cej.2020.124221).
- [51] Boix, G.; Troyano, J.; Garzón-Tovar, L.; Camur, C.; Bermejo, N.; Yazdi, A.; Piella, J.; Bastus, N. G.; Puentes, V. F.; Imaz, I.; et al. MOF-Beads Containing Inorganic Nanoparticles for the Simultaneous Removal of Multiple Heavy Metals from Water. *ACS Appl. Mater. Interfaces.* **2020**, *12*(9), 10554–10562. DOI: [10.1021/acsami.9b23206](https://doi.org/10.1021/acsami.9b23206).
- [52] Wu, J.; Zhou, J.; Zhang, S.; Alsaedi, A.; Hayat, T.; Li, J.; Song, Y. Efficient Removal of Metal Contaminants by EDTA Modified MOF from Aqueous Solutions. *J. Colloid Interface Sci.* **2019**, *555*, 403–412. DOI: [10.1016/j.jcis.2019.07.108](https://doi.org/10.1016/j.jcis.2019.07.108).
- [53] Esrafil, L.; Gharib, M.; Morsali, A. The Targeted Design of Dual-Functional Metal-Organic Frameworks (Df-MOFs) as Highly Efficient Adsorbents for Hg<sup>2+</sup> Ions: Synthesis for Purpose. *Dalton Trans.* **2019**, *48*, 17831–17839. DOI: [10.1039/C9DT03933C](https://doi.org/10.1039/C9DT03933C).
- [54] Zhao, M.; Huang, Z.; Wang, S.; Zhang, L.; Zhou, Y. Design of L-Cysteine Functionalized UiO-66 MOFs for Selective Adsorption of Hg(II) in Aqueous Medium. *ACS Appl. Mater. Interfaces.* **2019**, *11*(50), 46973–46983. DOI: [10.1021/acsami.9b17508](https://doi.org/10.1021/acsami.9b17508).
- [55] Sing, K. S. W.; Reporting Physisorption Data for Gas/Solid Systems with Special Reference to the Determination of Surface Area and Porosity (Provisional). *Pure Appl. Chem.* **1982**, *54*(11), 2201–2218. DOI: [10.1351/pac198254112201](https://doi.org/10.1351/pac198254112201).

- [56] Mohammadi, N.; Mousazadeh, B.; Hamoule, T. Synthesis and Characterization of  $\text{NH}_2\text{-SiO}_2\text{@Cu-MOF}$  as a High-Performance Adsorbent for Pb Ion Removal from Water Environment. *Environ. Dev. Sustain.* **2020**. DOI: [10.1007/s10668-020-00646-9](https://doi.org/10.1007/s10668-020-00646-9).
- [57] Wang, D.; Xiao, X.; Han, B.; Ni, W.; Gao, Y.; Li, L.; Xue, J. Adsorption of  $\text{Ni}^{2+}$  and  $\text{Cu}^{2+}$  from Aqueous Solution by Polyethyleneimine Impregnation of Metal-Organic Frameworks. *Nano.* **2020**, *15*(3), 2050029. DOI: [10.1142/S1793292020500290](https://doi.org/10.1142/S1793292020500290).
- [58] Shayegan, H.; Ali, G. A. M.; Safarifar, V. Amide-Functionalized Metal-Organic Framework for High Efficiency and Fast Removal of Pb(II) from Aqueous Solution. *J. Inorg. Organomet. Polym. Mater.* **2020**, *30*, 3170–3178. DOI: [10.1007/s10904-020-01474-0](https://doi.org/10.1007/s10904-020-01474-0).
- [59] Zhou, S.; Hu, C.; Xu, W.; Mo, X.; Zhang, P.; Liu, Y.; Tang, K. Fast Recovery of Au(III) and Ag(I) via Amine-Modified Zeolitic Imidazolate Framework-8. *Appl. Organomet. Chem.* **2020**, *34*(4), e5541. DOI: [10.1002/aoc.5541](https://doi.org/10.1002/aoc.5541).
- [60] Zhao, X.; Wang, Y.; Li, Y.; Xue, W.; Li, J.; Wu, H.; Zhang, Y.; Li, B.; Liu, W.; Gao, Z.; et al. Synergy Effect of Pore Structure and Amount of Carboxyl Site for Effective Removal of  $\text{Pb}^{2+}$  in Metal-Organic Frameworks. *J. Chem. Eng. Data.* **2019**, *64*(6), 2728–2735. DOI: [10.1021/acs.jced.9b00130](https://doi.org/10.1021/acs.jced.9b00130).
- [61] Lin, D.; Liu, X.; Huang, R.; Qi, W.; Su, R.; He, Z. One-Pot Synthesis of Mercapto Functionalized Zr-MOFs for the Enhanced Removal of  $\text{Hg}^{2+}$  Ions from Water. *Chem. Commun.* **2019**, *55*, 6775–6778. DOI: [10.1039/C9CC03481A](https://doi.org/10.1039/C9CC03481A).
- [62] Xie, Y.; Ye, G.; Peng, S.; Jiang, S.; Wang, Y.; Hu, X. Postsynthetic Functionalization of Water Stable Zirconium Metal Organic Frameworks for High Performance Copper Removal. *Analyst.* **2019**, *144*, 4552–4558. DOI: [10.1039/C9AN00981G](https://doi.org/10.1039/C9AN00981G).
- [63] Liu, F.; Xiong, W.; Feng, X.; Cheng, G.; Shi, L.; Chen, D.; Zhang, Y. Highly Recyclable Cysteine-modified Acid-resistant MOFs for Enhancing Hg (II) Removal from Water. *Environ. Technol.* **2020**, *41*(23), 3094–3104. DOI: [10.1080/09593330.2019.1598504](https://doi.org/10.1080/09593330.2019.1598504).
- [64] Zhao, M.; Huang, Z.; Wang, S.; Zhang, L.; Wang, C. Experimental and DFT Study on the Selective Adsorption Mechanism of Au(III) Using Amidinothiourea-Functionalized UiO-66- $\text{NH}_2$ . *Microporous Mesoporous Mater.* **2020**, *294*, 109905. DOI: [10.1016/j.micromeso.2019.109905](https://doi.org/10.1016/j.micromeso.2019.109905).
- [65] Wang, C.; Lin, G.; Zhao, J.; Wang, S.; Zhang, L.; Xi, Y.; Li, X.; Ying, Y. Highly Selective Recovery of Au(III) from Wastewater by Thioctic Acid Modified Zr-MOF: Experiment and DFT Calculation. *Chem. Eng. J.* **2020**, *380*, 122511. DOI: [10.1016/j.cej.2019.122511](https://doi.org/10.1016/j.cej.2019.122511).
- [66] Deng, -Y.-Y.; Xiao, X.-F.; Wang, D.; Han, B.; Gao, Y.; Xue, J.-L. Adsorption of Cr(VI) from Aqueous Solution by Ethylenediaminetetraacetic Acid-Chitosan-Modified Metal-Organic Framework. *J. Nanosci. Nanotechnol.* **2020**, *20*(3), 1660–1669. DOI: [10.1166/jnn.2020.17157](https://doi.org/10.1166/jnn.2020.17157).
- [67] Yuan, G.; Tian, Y.; Li, M.; Zeng, Y.; Tu, H.; Liao, J.; Yang, J.; Yang, Y.; Liu, N. Removal of Co(II) from Aqueous Solution with Functionalized Metal-Organic Frameworks (MOFs) Composite. *J. Radioanal. Nucl. Chem.* **2019**, *322*, 827–838. DOI: [10.1007/s10967-019-06764-7](https://doi.org/10.1007/s10967-019-06764-7).
- [68] Fu, L.; Wang, S.; Lin, G.; Zhang, L.; Liu, Q.; Zhou, H.; Kang, C.; Wan, S.; Li, H.; Wen, S. Post-Modification of UiO-66- $\text{NH}_2$  by Resorcinol Aldehyde for Selective Removal of Pb(II) in Aqueous Media. *J. Cleaner Prod.* **2019**, *229*, 470–479. DOI: [10.1016/j.jclepro.2019.05.043](https://doi.org/10.1016/j.jclepro.2019.05.043).
- [69] Wu, H.; Chi, F.; Zhang, S.; Wen, J.; Xiong, J.; Hu, S. Control of Pore Chemistry in Metal-Organic Frameworks for Selective Uranium Extraction from Seawater. *Microporous Mesoporous Mater.* **2019**, *288*, 109567. DOI: [10.1016/j.micromeso.2019.109567](https://doi.org/10.1016/j.micromeso.2019.109567).
- [70] Yuan, G.; Tu, H.; Li, M.; Liu, J.; Zhao, C.; Liao, J.; Yang, Y.; Yang, J.; Liu, N. Glycine Derivative-Functionalized Metal-Organic Framework (MOF) Materials for Co(II) Removal from Aqueous Solution. *Appl. Surf. Sci.* **2019**, *466*, 903–910. DOI: [10.1016/j.apsusc.2018.10.129](https://doi.org/10.1016/j.apsusc.2018.10.129).
- [71] Xiong, C.; Wang, S.; Hu, P.; Huang, L.; Xue, C.; Yang, Z.; Zhou, X.; Wang, Y.; Ji, H. Efficient Selective Removal of Pb(II) by Using 6-Aminothiouracil-Modified Zr-Based Organic Frameworks: From Experiments to Mechanisms. *ACS Appl. Mater. Interfaces.* **2020**, *12*(6), 7162–7178. DOI: [10.1021/acsami.9b19516](https://doi.org/10.1021/acsami.9b19516).
- [72] Zhao, J.; Wang, C.; Wang, S.; Zhou, Y. Experimental and DFT Study of Selective Adsorption Mechanisms of Pb(II) by UiO-66- $\text{NH}_2$  Modified with 1,8-Dihydroxyanthraquinone. *J. Ind. Eng. Chem.* **2020**, *83*, 111–122. DOI: [10.1016/j.jiec.2019.11.019](https://doi.org/10.1016/j.jiec.2019.11.019).
- [73] Xiong, Y.; Gao, Y.; Guo, X.; Wang, Y.; Su, X.; Sun, X. Water-Stable Metal-Organic Framework Material with Uncoordinated Terpyridine Site for Selective Th(IV)/Ln(III) Separation. *ACS Sustainable Chem. Eng.* **2019**, *7*(3), 3120–3126. DOI: [10.1021/acssuschemeng.8b04875](https://doi.org/10.1021/acssuschemeng.8b04875).
- [74] Li, L.; Ma, W.; Shen, S.; Huang, H.; Bai, Y.; Liu, H. A Combined Experimental and Theoretical Study on the Extraction of Uranium by Amino-Derived Metal-Organic Frameworks through Post-Synthetic Strategy. *ACS Appl. Mater. Interfaces.* **2016**, *8*(45), 31032–31041. DOI: [10.1021/acsami.6b11332](https://doi.org/10.1021/acsami.6b11332).
- [75] Geisse, A. R.; Ngule, C. M.; Genna, D. T. Removal of Lead Ions from Water Using Thiophene-Functionalized Metal-Organic Frameworks. *Chem. Commun.* **2020**, *56*, 237–240. DOI: [10.1039/C9CC09022C](https://doi.org/10.1039/C9CC09022C).
- [76] Karimi, M. A.; Masrouri, H.; Karami, H.; Andishgar, S.; Mirbagheri, M. A.; Pourshamsi, T. Highly Efficient Removal of Toxic Lead Ions from Aqueous Solutions Using a New Magnetic Metal-Organic Framework Nanocomposite. *J. Chin. Chem. Soc.* **2019**, *66*(10), 1327–1335. DOI: [10.1002/jccs.201800378](https://doi.org/10.1002/jccs.201800378).
- [77] Zhang, J.; Xiong, Z.; Li, C.; Wu, C. Exploring a Thiol-Functionalized MOF for Elimination of Lead and Cadmium from Aqueous Solution. *J. Mol. Liq.* **2016**, *221*, 43–50. DOI: [10.1016/j.molliq.2016.05.054](https://doi.org/10.1016/j.molliq.2016.05.054).
- [78] Yang, P.; Shu, Y.; Zhuang, Q.; Li, Y.; Gu, J. A Robust MOF-based Trap with High-density Active Alkyl Thiol for the Super-efficient Capture of Mercury. *Chem. Commun.* **2019**, *55*(86), 12972–12975. DOI: [10.1039/C9CC06255F](https://doi.org/10.1039/C9CC06255F).
- [79] Li, L.; Xu, Y.; Zhong, D.; Zhong, N. CTAB-Surface-Functionalized Magnetic MOF@MOF Composite Adsorbent for Cr(VI) Efficient Removal from Aqueous Solution. *Colloids Surf., A.* **2020**, *586*, 124255. DOI: [10.1016/j.colsurfa.2019.124255](https://doi.org/10.1016/j.colsurfa.2019.124255).
- [80] He, X.; Deng, F.; Shen, T.; Yang, L.; Chen, D.; Luo, J.; Luo, X.; Min, X.; Wang, F. Exceptional Adsorption of Arsenic by Zirconium Metal-Organic Frameworks: Engineering Exploration and Mechanism Insight. *J. Colloid Interface Sci.* **2019**, *539*, 223–234. DOI: [10.1016/j.jcis.2018.12.065](https://doi.org/10.1016/j.jcis.2018.12.065).
- [81] He, X.; Min, X.; Luo, X. Efficient Removal of Antimony(III, V) from Contaminated Water by Amino Modification of a Zirconium Metal-Organic Framework with Mechanism Study. *J. Chem. Eng. Data.* **2017**, *62*(4), 1519–1529. DOI: [10.1021/acs.jced.7b00010](https://doi.org/10.1021/acs.jced.7b00010).
- [82] Qi, P.; Luo, R.; Pichler, T.; Zeng, J.; Wang, Y.; Fan, Y.; Sui, K. Development of a Magnetic Core-Shell  $\text{Fe}_3\text{O}_4\text{@TA@UiO-66}$  Microsphere for Removal of Arsenic(III) and Antimony(III) from Aqueous Solution. *J. Hazard. Mater.* **2019**, *378*, 120721. DOI: [10.1016/j.jhazmat.2019.05.114](https://doi.org/10.1016/j.jhazmat.2019.05.114).
- [83] Huang, Z.; Zhao, M.; Wang, S.; Dai, L.; Zhang, L.; Wang, C. Selective Recovery of Gold Ions in Aqueous Solutions by a Novel Trithiocyanuric-Zr Based MOFs Adsorbent. *J. Mol. Liq.* **2020**, *298*, 112090. DOI: [10.1016/j.molliq.2019.112090](https://doi.org/10.1016/j.molliq.2019.112090).
- [84] Elsaidi, S. K.; Sinnwell, M. A.; Devaraj, A.; Droubay, T. C.; Nie, Z.; Murugesan, V.; Mcgrail, B. P.; Thallapally, P. K. Extraction of Rare Earth Elements Using Magnetite@MOF Composites. *J. Mater. Chem. A.* **2018**, *6*, 18438–18443. DOI: [10.1039/C8TA04750B](https://doi.org/10.1039/C8TA04750B).
- [85] Lee, Y.-R.; Yu, K.; Ravi, S.; Ahn, W.-S. Selective Adsorption of Rare Earth Elements over Functionalized Cr-MIL-101. *ACS Appl. Mater. Interfaces.* **2018**, *10*(28), 23918–23927. DOI: [10.1021/acsami.8b07130](https://doi.org/10.1021/acsami.8b07130).
- [86] Zhao, L.; Azhar, M. R.; Li, X.; Duan, X.; Sun, H.; Wang, S.; Fang, X. Adsorption of Cerium(III) by HKUST-1 Metal-Organic Framework from Aqueous Solution. *J. Colloid Interface Sci.* **2019**, *542*, 421–428. DOI: [10.1016/j.jcis.2019.01.117](https://doi.org/10.1016/j.jcis.2019.01.117).
- [87] Abdelhameed, R. M.; Ismail, R. A.; El-Naggar, M.; Zari, E. S.; Abdelaziz, R.; El Sayed, M. T. Post-Synthetic Modification of MIL-125 with Bis-Quinoline Mannich Bases for Removal of

- Heavy Metals from Wastewater. *Microporous Mesoporous Mater.* **2019**, 279, 26–36. DOI: [10.1016/j.micromeso.2018.12.018](https://doi.org/10.1016/j.micromeso.2018.12.018).
- [88] Yang, L. X.; Feng, X. F.; Yin, W. H.; Tao, Y.; Wu, H. Q.; Li, J. Q.; Ma, L. F.; Luo, F. Metal-Organic Framework Containing Both Azo and Amide Groups for Effective U(VI) Removal. *J. Solid State Chem.* **2018**, 265, 148–154. DOI: [10.1016/j.jssc.2018.05.040](https://doi.org/10.1016/j.jssc.2018.05.040).
- [89] Tao, Y.; Yang, L. X.; Li, J. H.; Feng, X. F.; Yin, W. H.; Wu, H. Q.; Li, J. Q.; Luo, F.; New Azo, A. Metal-Organic Framework Showing Polycatenated 3D Array and Ultrahigh U(VI) Removal. *J. Solid State Chem.* **2018**, 266, 244–249. DOI: [10.1016/j.jssc.2018.07.027](https://doi.org/10.1016/j.jssc.2018.07.027).
- [90] Liu, J.; Liu, T.; Wang, C.; Yin, X.; Xiong, Z. Introduction of Amidoxime Groups into Metal-Organic Frameworks to Synthesize MIL-53(Al)-AO for Enhanced U(VI) Sorption. *J. Mol. Liq.* **2017**, 242, 531–536. DOI: [10.1016/j.molliq.2017.07.024](https://doi.org/10.1016/j.molliq.2017.07.024).
- [91] Feng, Y.; Jiang, H.; Li, S.; Wang, J.; Jing, X.; Wang, Y.; Chen, M. Metal-Organic Frameworks HKUST-1 for Liquid-Phase Adsorption of Uranium. *Colloids Surf., A*. **2013**, 431, 87–92. DOI: [10.1016/j.colsurfa.2013.04.032](https://doi.org/10.1016/j.colsurfa.2013.04.032).
- [92] Li, J. Q.; Gong, L.; Feng, X. F.; Zhang, L.; Wu, H. Q.; Yan, C. S.; Xiong, Y. Y.; Gao, H. Y.; Luo, F. Direct Extraction of U(VI) from Alkaline Solution and Seawater via Anion Exchange by Metal-Organic Framework. *Chem. Eng. J.* **2017**, 316, 154–159. DOI: [10.1016/j.cej.2017.01.046](https://doi.org/10.1016/j.cej.2017.01.046).
- [93] Zhang, J.; Zhang, H.; Liu, Q.; Song, D.; Li, R.; Liu, P.; Wang, J. Diaminomaleonitrile Functionalized Double-Shelled Hollow MIL-101(Cr) for Selective Removal of Uranium from Simulated Seawater. *Chem. Eng. J.* **2019**, 368, 951–958. DOI: [10.1016/j.cej.2019.02.096](https://doi.org/10.1016/j.cej.2019.02.096).
- [94] Wu, Y.; Pang, H.; Yao, W.; Wang, X.; Yu, S.; Yu, Z.; Wang, X. Synthesis of Rod-Like Metal-Organic Framework (MOF-5) Nanomaterial for Efficient Removal of U(VI): Batch Experiments and Spectroscopy Study. *Sci. Bull.* **2018**, 63(13), 831–839. DOI: [10.1016/j.scib.2018.05.021](https://doi.org/10.1016/j.scib.2018.05.021).
- [95] Bai, Z.-Q.; Yuan, L.-Y.; Zhu, L.; Liu, Z.-R.; Chu, S.-Q.; Zheng, L.-R.; Zhang, J.; Chai, Z.-F.; Shi, W.-Q. Introduction of Amino Groups into Acid-Resistant MOFs for Enhanced U(VI) Sorption. *J. Mater. Chem. A*. **2015**, 3, 525–534. DOI: [10.1039/C4TA04878D](https://doi.org/10.1039/C4TA04878D).
- [96] Wang, L. L.; Luo, F.; Dang, L. L.; Li, J. Q.; Wu, X. L.; Liu, S. J.; Luo, M. B. Ultrafast High-Performance Extraction of Uranium from Seawater without Pretreatment Using an Acylamide- and Carboxyl-Functionalized Metal-Organic Framework. *J. Mater. Chem. A*. **2015**, 3, 13724–13730. DOI: [10.1039/C5TA01972A](https://doi.org/10.1039/C5TA01972A).
- [97] Carboni, M.; Abney, C. W.; Liu, S.; Lin, W. Highly Porous and Stable Metal-Organic Frameworks for Uranium Extraction. *Chem. Sci.* **2013**, 4, 2396–2402. DOI: [10.1039/C3SC50230A](https://doi.org/10.1039/C3SC50230A).
- [98] Alqadami, A. A.; Naushad, M.; Alotman, Z. A.; Ghfar, A. A. Novel Metal-Organic Framework (MOF) Based Composite Material for the Sequestration of U(VI) and Th(IV) Metal Ions from Aqueous Environment. *ACS Appl. Mater. Interfaces*. **2017**, 9(41), 36026–36037. DOI: [10.1021/acsami.7b10768](https://doi.org/10.1021/acsami.7b10768).
- [99] Falaise, C.; Volkringer, C.; Giovine, R.; Prelot, B.; Huve, M.; Loiseau, T. Capture of Actinides (Th<sup>4+</sup>, [UO<sub>2</sub>]<sup>2+</sup>) and Surrogating Lanthanide (Nd<sup>3+</sup>) in Porous Metal-Organic Framework MIL-100(Al) from Water: Selectivity and Imaging of Embedded Nanoparticles. *Dalton Trans.* **2017**, 46, 12010–12014. DOI: [10.1039/C7DT02155K](https://doi.org/10.1039/C7DT02155K).
- [100] Huang, Z.-H.; Zheng, X.; Lv, W.; Wang, M.; Yang, Q.-H.; Kang, F. Adsorption of Lead(II) Ions from Aqueous Solution on Low-Temperature Exfoliated Graphene Nanosheets. *Langmuir*. **2011**, 27(12), 7558–7562. DOI: [10.1021/la200606r](https://doi.org/10.1021/la200606r).
- [101] Tan, P.; Sun, J.; Hu, Y.; Fang, Z.; Bi, Q.; Chen, Y.; Cheng, J. Adsorption of Cu<sup>2+</sup>, Cd<sup>2+</sup> and Ni<sup>2+</sup> from Aqueous Single Metal Solutions on Graphene Oxide Membranes. *J. Hazard. Mater.* **2015**, 297, 251–260. DOI: [10.1016/j.jhazmat.2015.04.068](https://doi.org/10.1016/j.jhazmat.2015.04.068).
- [102] Li, Y.-H.; Ding, J.; Luan, Z.; Di, Z.; Zhu, Y.; Xu, C.; Wu, D.; Wei, B. Competitive Adsorption of Pb<sup>2+</sup>, Cu<sup>2+</sup> and Cd<sup>2+</sup> Ions from Aqueous Solutions by Multiwalled Carbon Nanotubes. *Carbon*. **2003**, 41(14), 2787–2792. DOI: [10.1016/S0008-6223\(03\)00392-0](https://doi.org/10.1016/S0008-6223(03)00392-0).
- [103] Mullick, A.; Moulik, S.; Bhattacharjee, S. Removal of Hexavalent Chromium from Aqueous Solutions by Low-Cost Rice Husk-Based Activated Carbon: Kinetic and Thermodynamic Studies. *Indian Chem. Eng.* **2018**, 60(1), 58–71. DOI: [10.1080/00194506.2017.1288173](https://doi.org/10.1080/00194506.2017.1288173).
- [104] Li, K.; Zheng, Z.; Li, Y. Characterization and Lead Adsorption Properties of Activated Carbons Prepared from Cotton Stalk by One-Step H<sub>3</sub>PO<sub>4</sub> Activation. *J. Hazard. Mater.* **2010**, 181(1–3), 440–447. DOI: [10.1016/j.jhazmat.2010.05.030](https://doi.org/10.1016/j.jhazmat.2010.05.030).
- [105] Ma, L.; Wang, Q.; Islam, S. M.; Liu, Y.; Ma, S.; Kanatzidis, M. G. Highly Selective and Efficient Removal of Heavy Metals by Layered Double Hydroxide Intercalated with the MoS<sub>4</sub><sup>2-</sup> Ion. *J. Am. Chem. Soc.* **2016**, 138(8), 2858–2866. DOI: [10.1021/jacs.6b00110](https://doi.org/10.1021/jacs.6b00110).
- [106] Qiao, -X.-X.; Liu, G.-F.; Wang, J.-T.; Zhang, Y.-Q.; Lü, J. Highly Efficient and Selective Removal of Lead Ions from Aqueous Solutions by Conjugated Microporous Polymers with Functionalized Heterogeneous Pores. *Cryst. Growth Des.* **2020**, 20(1), 337–344. DOI: [10.1021/acs.cgd.9b01265](https://doi.org/10.1021/acs.cgd.9b01265).
- [107] Meri-Bofi, L.; Royuela, S.; Zamora, F.; Ruiz-González, M. L.; Segura, J. L.; Muñoz-Olivas, R.; Mancheño, M. J. Thiol Grafted Imine-Based Covalent Organic Frameworks for Water Remediation through Selective Removal of Hg(II). *J. Mater. Chem. A*. **2017**, 5, 17973–17981. DOI: [10.1039/C7TA05588A](https://doi.org/10.1039/C7TA05588A).
- [108] Wang, Z.; Tan, K.; Cai, J.; Hou, S.; Wang, Y.; Jiang, P.; Liang, M. Silica Oxide Encapsulated Natural Zeolite for High Efficiency Removal of Low Concentration Heavy Metals in Water. *Colloids Surf., A*. **2019**, 561, 388–394. DOI: [10.1016/j.colsurfa.2018.10.065](https://doi.org/10.1016/j.colsurfa.2018.10.065).
- [109] Hu, B.; Guo, X.; Zheng, C.; Song, G.; Chen, D.; Zhu, Y.; Song, X.; Sun, Y. Plasma-Enhanced Amidoxime/Magnetic Graphene Oxide for Efficient Enrichment of U(VI) Investigated by EXAFS and Modeling Techniques. *Chem. Eng. J.* **2019**, 357, 66–74. DOI: [10.1016/j.cej.2018.09.140](https://doi.org/10.1016/j.cej.2018.09.140).
- [110] Xie, L.; Zhong, Y.; Xiang, R.; Fu, G.; Xu, Y.; Cheng, Y.; Liu, Z.; Wen, T.; Zhao, Y.; Liu, X. Sono-Assisted Preparation of Fe(II)-Al(III) Layered Double Hydroxides and Their Application for Removing Uranium (VI). *Chem. Eng. J.* **2017**, 328, 574–584. DOI: [10.1016/j.cej.2017.07.051](https://doi.org/10.1016/j.cej.2017.07.051).
- [111] Tian, G.; Geng, J.; Jin, Y.; Wang, C.; Li, S.; Chen, Z.; Wang, H.; Zhao, Y.; Li, S. Sorption of Uranium(VI) Using Oxime-Grafted Ordered Mesoporous Carbon CMK-5. *J. Hazard. Mater.* **2011**, 190(1–3), 442–450. DOI: [10.1016/j.jhazmat.2011.03.066](https://doi.org/10.1016/j.jhazmat.2011.03.066).
- [112] Cheng, L.; Zhai, L.; Liao, W.; Huang, X.; Niu, B.; Yu, S. An Investigation on the Behaviors of Thorium(IV) Adsorption onto Chrysotile Nanotubes. *J. Environ. Chem. Eng.* **2014**, 2(3), 1236–1242. DOI: [10.1016/j.jece.2014.05.014](https://doi.org/10.1016/j.jece.2014.05.014).
- [113] Morsy, A. M. A.; Performance of Magnetic Talc Titanium Oxide Composite for Thorium Ions Adsorption from Acidic Solution. *Environ. Technol. Innovations*. **2017**, 8, 399–410. DOI: [10.1016/j.eti.2017.09.004](https://doi.org/10.1016/j.eti.2017.09.004).
- [114] Wang, Z.; Brown, A. T.; Tan, K.; Chabal, Y. J.; Balkus, J. J.; K. Selective Extraction of Thorium from Rare Earth Elements Using Wrinkled Mesoporous Carbon. *J. Am. Chem. Soc.* **2018**, 140(44), 14735–14739. DOI: [10.1021/jacs.8b07610](https://doi.org/10.1021/jacs.8b07610).
- [115] Tchounwou, P. B.; Yedjou, C. G.; Patlolla, A. K.; Sutton, D. J. Heavy Metal Toxicity and the Environment. In *Molecular, Clinical and Environmental Toxicology*; Luch, A., Ed.; Springer: Basel, **2012**; pp 133–164. DOI: [10.1007/978-3-7643-8340-4\\_6](https://doi.org/10.1007/978-3-7643-8340-4_6).
- [116] Akbal, F.; Camci, S. Comparison of Electrocoagulation and Chemical Coagulation for Heavy Metal Removal. *Chem. Eng. Technol.* **2010**, 33(10), 1655–1664. DOI: [10.1002/ceat.201000091](https://doi.org/10.1002/ceat.201000091).
- [117] Chen, Q.; Luo, Z.; Hills, C.; Xue, G.; Tyrer, M. Precipitation of Heavy Metals from Wastewater Using Simulated Flue Gas: Sequential Additions of Fly Ash, Lime and Carbon Dioxide. *Water Res.* **2009**, 43(10), 2605–2614. DOI: [10.1016/j.watres.2009.03.007](https://doi.org/10.1016/j.watres.2009.03.007).
- [118] Trivunac, K.; Stevanovic, S. Removal of Heavy Metal Ions from Water by Complexation-Assisted Ultrafiltration. *Chemosphere*. **2006**, 64(3), 486–491. DOI: [10.1016/j.chemosphere.2005.11.073](https://doi.org/10.1016/j.chemosphere.2005.11.073).
- [119] Lee, B. G.; Lee, H. J.; Shin, D. Y. Effect of Solvent Extraction on Removal of Heavy Metal Ions Using Lignocellulosic Fiber. *Mater. Sci. Forum*. **2005**, 486–487, 574–577.
- [120] Yang, Y.; Wang, G.; Deng, Q.; Wang, H.; Zhang, Y.; Ng, D. H. L.; Zhao, H. Enhanced Photocatalytic Activity of Hierarchical Structure TiO<sub>2</sub> Hollow Spheres with Reactive (001) Facets for the

- Removal of Toxic Heavy Metal Cr(VI). *RSC Adv.* **2014**, *4*, 34577–34583. DOI: [10.1039/C4RA04787G](https://doi.org/10.1039/C4RA04787G).
- [121] Qdais, H. A.; Moussa, H. Removal of Heavy Metals from Wastewater by Membrane Processes: A Comparative Study. *Desalination*. **2004**, *164*(2), 105–110. DOI: [10.1016/S0011-9164\(04\)00169-9](https://doi.org/10.1016/S0011-9164(04)00169-9).
- [122] Fu, F.; Han, W.; Tang, B.; Hu, M.; Cheng, Z. Insights into Environmental Remediation of Heavy Metal and Organic Pollutants: Simultaneous Removal of Hexavalent Chromium and Dye from Wastewater by Zero-Valent Iron with Ligand-Enhanced Reactivity. *Chem. Eng. J.* **2013**, *232*, 534–540. DOI: [10.1016/j.cej.2013.08.014](https://doi.org/10.1016/j.cej.2013.08.014).
- [123] Sahu, J. N.; Agarwal, S.; Meikap, B. C.; Biswas, M. N. Performance of a Modified Multi-Stage Bubble Column Reactor for Lead(II) and Biological Oxygen Demand Removal from Wastewater Using Activated Rice Husk. *J. Hazard. Mater.* **2009**, *161*(1), 317–324. DOI: [10.1016/j.jhazmat.2008.03.094](https://doi.org/10.1016/j.jhazmat.2008.03.094).
- [124] Flora, G.; Gupta, D.; Tiwari, A. Toxicity of Lead: A Review with Recent Updates. *Interdiscip. Toxicol.* **2012**, *5*(2), 47–58. DOI: [10.2478/v10102-012-0009-2](https://doi.org/10.2478/v10102-012-0009-2).
- [125] Park, D.; Yun, Y.-S.; Jo, J. H.; Park, J. M. Mechanism of Hexavalent Chromium Removal by Dead Fungal Biomass of *Aspergillus Niger*. *Water Res.* **2005**, *39*(4), 533–540. DOI: [10.1016/j.watres.2004.11.002](https://doi.org/10.1016/j.watres.2004.11.002).
- [126] Gupta, N. K.; Gupta, A.; Ramteke, P.; Sahoo, H.; Sengupta, A. Biosorption-A Green Method for the Preconcentration of Rare Earth Elements (Rees) from Waste Solutions: A Review. *J. Mol. Liq.* **2019**, *274*, 148–164. DOI: [10.1016/j.molliq.2018.10.134](https://doi.org/10.1016/j.molliq.2018.10.134).
- [127] Ciupka, J.; Cao-Dolg, X.; Wiebke, J.; Dolg, M. Computational Study of Lanthanide(III) Hydration. *Phys. Chem. Chem. Phys.* **2010**, *12*, 13215–13223. DOI: [10.1039/C0CP00639D](https://doi.org/10.1039/C0CP00639D).
- [128] Chen, L.; Bai, Z.; Zhu, L.; Zhang, L.; Cai, Y.; Li, Y.; Liu, W.; Wang, Y.; Chen, L.; Diwu, J.; et al. Ultrafast and Efficient Extraction of Uranium from Seawater Using an Amidoxime Appended Metal-Organic Framework. *ACS Appl. Mater. Interfaces*. **2017**, *9*(38), 32446–32451. DOI: [10.1021/acsami.7b12396](https://doi.org/10.1021/acsami.7b12396).
- [129] Guo, X.-G.; Qiu, S.; Chen, X.; Gong, Y.; Sun, X. Postsynthesis Modification of a Metallosalen-Containing Metal-Organic Framework for Selective Th(IV)/Ln(III) Separation. *Inorg. Chem.* **2017**, *56*(20), 12357–12361. DOI: [10.1021/acs.inorgchem.7b01835](https://doi.org/10.1021/acs.inorgchem.7b01835).